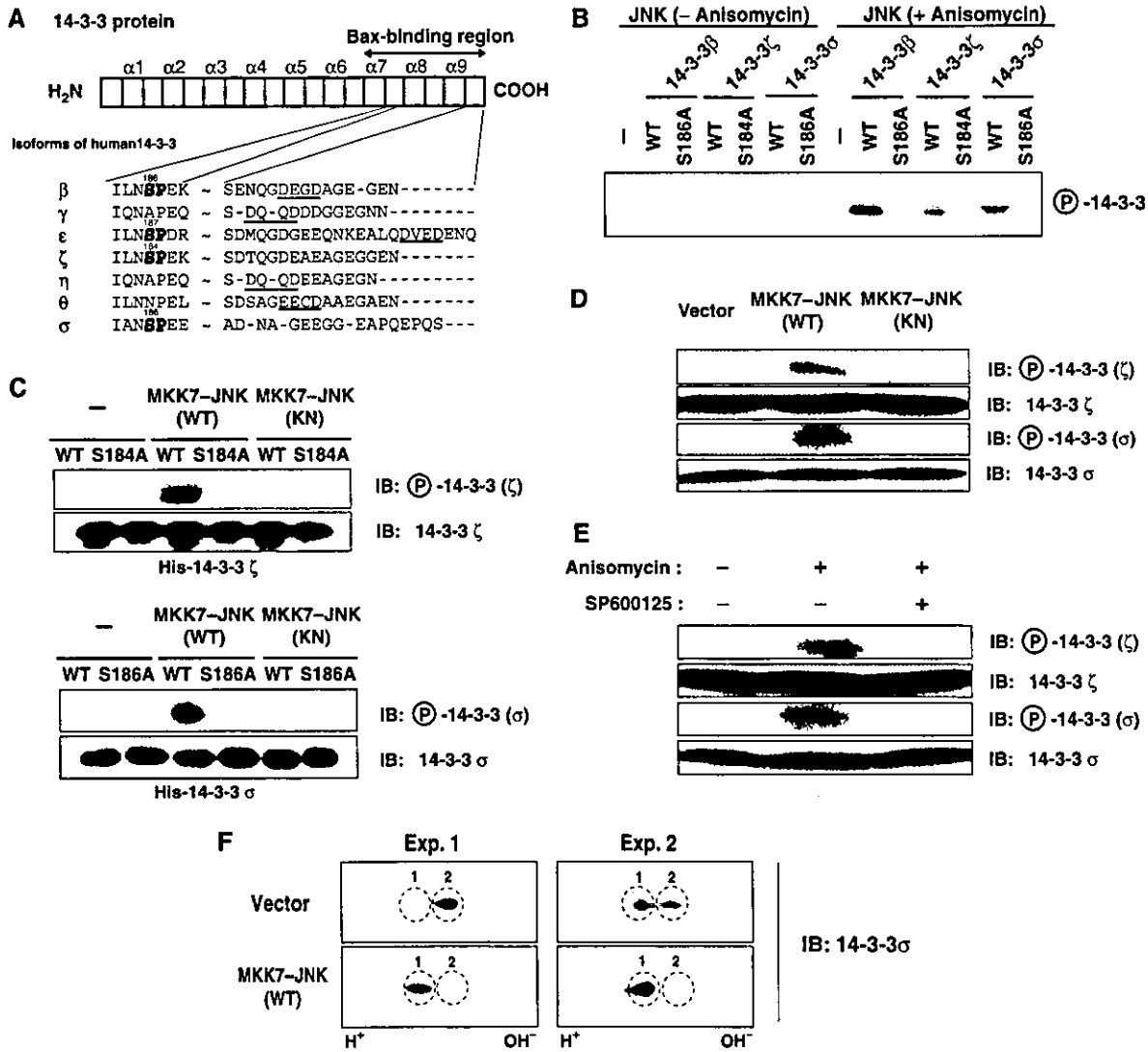

Figure 4 JNK phosphorylates 14-3-3ζ and 14-3-3σ both *in vitro* and *in vivo*. (**A**) Schematic representation of the structure of human 14-3-3 proteins and the amino-acid sequences surrounding putative JNK phosphorylation sites (SP, shown in bold) and caspase-3 cleavage sites ((D/E)XXD, underlined) in the Bax-binding region of the indicated isoforms. The numbers indicate the position of putative phosphorylation sites. (**B**) COS-1 cells were transfected for 24 h with an expression vector for Flag-tagged JNK and then incubated for 1 h in the absence or presence of anisomycin (10 μg/ml). Flag–JNK was immunoprecipitated from cell lysates with antibodies to Flag and incubated with the indicated recombinant His_6-tagged 14-3-3 proteins (WT or Ser→Ala mutants) in the presence of [γ-^{32}P]ATP. The amount of JNK immunoprecipitated from anisomycin-treated cell extracts was comparable to that from untreated cell extracts under the conditions used in this *in vitro* kinase assay (data not shown). Phosphorylation of 14-3-3 proteins was detected by electrophoresis and autoradiography. (**C**) Recombinant His_6-tagged 14-3-3 proteins (WT or mutant) were incubated with or without recombinant MKK7–JNK(WT or KN) in the presence of ATP and were then subjected to immunoblot analysis with antibodies specific for 14-3-3ζ or 14-3-3ζ phosphorylated on Ser^{184} (upper panels) or for 14-3-3σ or 14-3-3σ phosphorylated on Ser^{186} (lower panels). (**D**) HCT116 cells were transfected for 1 day with an expression vector for MKK7–JNK(WT or KN) or the corresponding empty vector, after which cell lysates were subjected to immunoblot analysis with the antibodies described in (C). (**E**) HCT116 cells were incubated first for 30 min with or without 20 μM SP600125 and then for 3 h in the presence or absence of anisomycin (10 μg/ml). Cell lysates were then subjected to immunoblot analysis as described in (D). (**F**) HCT116 cells were transfected for 1 day with an expression vector for MKK7–JNK(WT) or the corresponding empty vector, after which cell lysates were subjected to two-dimensional gel electrophoresis and immunoblot analysis with anti-14-3-3σ antibody. Two typical results (Exp. 1 and Exp. 2) are shown. The ratio between Spot 1 and Spot 2 in control cells varied among experiments, but expression of MKK7–JNK (WT) repeatedly increased Spot 1 and abolished Spot 2.

first examined whether JNK is capable of phosphorylating 14-3-3 proteins. Active JNK immunoprecipitated from anisomycin-treated COS-1 cell extracts efficiently phosphorylated recombinant His-tagged 14-3-3β, 14-3-3ζ and 14-3-3σ in an *in vitro* kinase assay (Figure 4B). JNK immunoprecipitates prepared from untreated cells did not phosphorylate recombinant 14-3-3 proteins, confirming that the kinase activity of JNK was responsible for this phosphorylation. Mutant proteins in which Ser-184 of 14-3-3ζ or Ser-186 of 14-3-3β or 14-3-3σ was replaced with alanine were not phosphorylated by the active JNK immunoprecipitated from anisomycin-treated cells (Figure 4B), indicating that these serine residues are the JNK-mediated phosphorylation sites *in vitro*.

To further indicate that Ser-184 of 14-3-3ζ and Ser-186 of 14-3-3σ are phosphorylated by JNK, we prepared antibodies to phosphopeptides corresponding to these phosphorylation

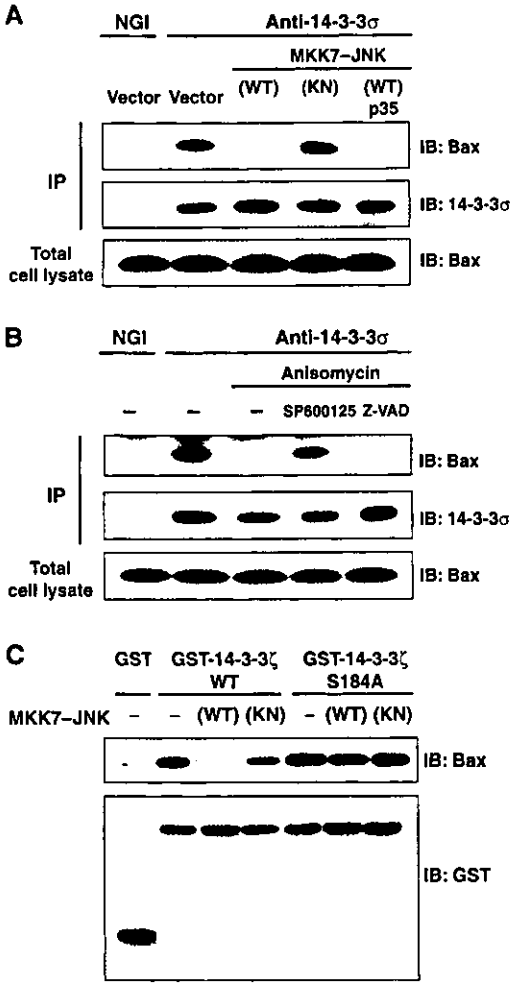

Figure 5 JNK promotes dissociation of Bax from 14-3-3 proteins. (**A**) HCT116 cells were transfected for 24 h with expression vectors for GFP, MKK7-JNK(WT or KN) and p35, as indicated. Cell lysates were then subjected either to immunoblot analysis with antibodies to Bax or to immunoprecipitation (IP) with antibodies to 14-3-3σ (or to normal goat IgG (NGI) precipitation); the resulting precipitates were subjected to immunoblot analysis with antibodies to 14-3-3σ and to Bax. (**B**) HCT116 cells were incubated first for 30 min with or without 20 μM SP600125 or 100 μM Z-VAD-CH_2DCB and then for 3 h in the presence or absence of anisomycin (10 μg/ml). Cell lysates were then subjected to immunoprecipitation and immunoblot analysis as described in (A). (**C**) Equal amounts of recombinant GST-14-3-3ζ (WT or Ser^{184}→Ala mutant) or GST alone were incubated with or without recombinant MKK7-JNK(WT or KN) in the presence of ATP for 30 min, and the GST proteins were precipitated with glutathione-sepharose beads. The beads were then incubated with HeLa cell lysates, and subjected to immunoblot analysis with antibodies to Bax or to GST.

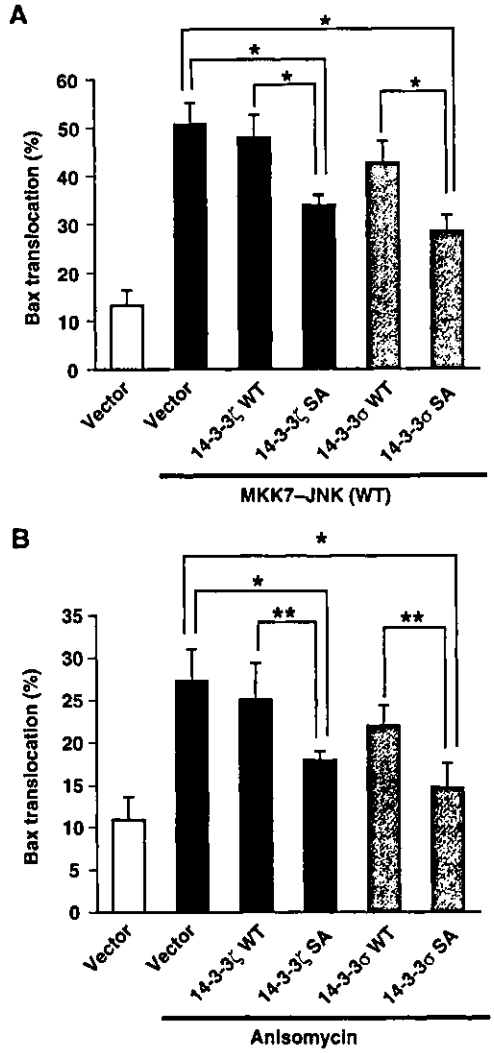

Figure 6 14-3-3 mutants inhibit JNK-induced Bax translocation to mitochondria. (**A**) COS-1 cells were transfected for 16 h with expression vectors for GFP-Bax and p35 together with those for MKK7-JNK(WT) and either 14-3-3ζ or 14-3-3σ. The percentage of cells exhibiting GFP-Bax localization to the mitochondria was then determined. Data are means±s.d. of values obtained from five fields of 30–150 cells in each of three independent experiments (*$P<0.0005$). (**B**) COS-1 cells were transfected for 11.5 h with expression vectors for GFP-Bax, p35 and either 14-3-3ζ or 14-3-3σ, and were incubated for 6 h in the presence or absence of anisomycin (10 μg/ml). The percentage of cells in which GFP-Bax was localized to the mitochondria was then determined and shown as in (A) (*$P<0.0005$ and **$P<0.005$).

sites. The anti-phospho-Ser^{184}-14-3-3ζ and anti-phospho-Ser^{186}-14-3-3σ antibodies recognized recombinant 14-3-3 proteins (14-3-3ζ and σ) that had been phosphorylated by recombinant MKK7-JNK(WT), but not those incubated with MKK7-JNK(KN) (Figure 4C). Moreover, these antibodies did not react with the Ser→Ala (SA) mutants of the corresponding 14-3-3 proteins, confirming that they specifically recognize phosphorylated 14-3-3 proteins at these serine residues.

JNK phosphorylates 14-3-3ζ at Ser-184 and 14-3-3σ at Ser-186 in vivo

To determine whether JNK also phosphorylates 14-3-3 *in vivo*, we examined the phosphorylation status of 14-3-3 proteins with the anti-phospho-14-3-3 antibodies. We used HCT116 cells in which ζ and σ isoforms of 14-3-3 are expressed endogenously. Expression of MKK7-JNK(WT), but not MKK7-JNK(KN), in HCT116 cells increased the bands reactive to the antibodies raised against phosphopeptides for 14-3-3ζ at Ser-184 and 14-3-3σ at Ser-186 (Figure 4D), suggesting that endogenous 14-3-3 proteins became phosphorylated upon JNK activation. We then addressed whether the phosphorylation of 14-3-3 is induced by cellular stresses. Exposure of HCT116 cells to anisomycin induced the phosphorylation of 14-3-3 proteins, revealed by the antibodies for 14-3-3ζ at Ser-184 and 14-3-3σ at Ser-186 (Figure 4E). The concentration of anisomycin required for phosphorylation of 14-3-3 was similar to that required for

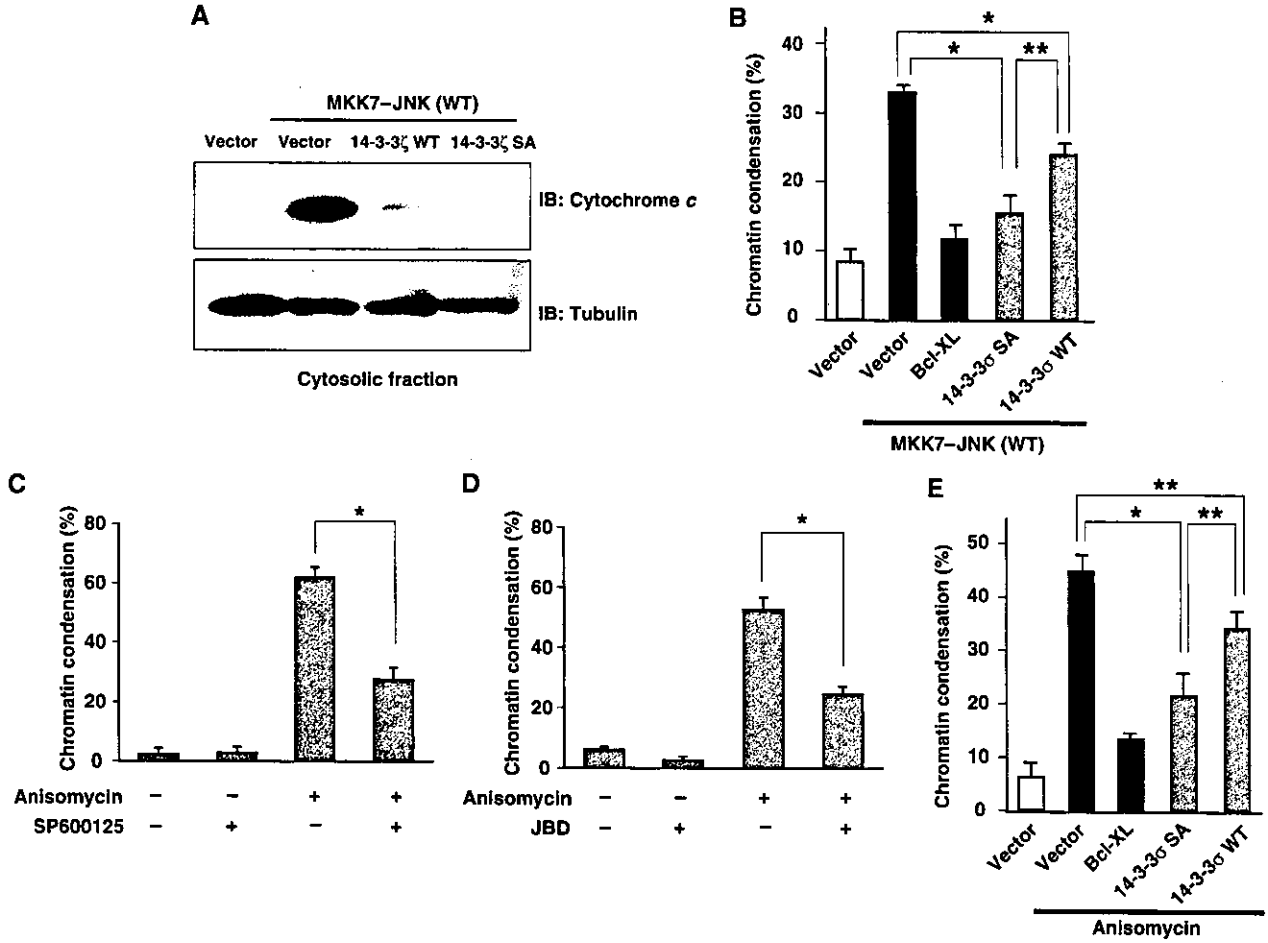

Figure 7 14-3-3 mutants inhibit JNK-induced cell death. (**A**) COS-1 cells were transfected for 20 h with expression vectors for GFP, MKK7-JNK(WT), and either 14-3-3ζ WT or 14-3-3ζ S184A, as indicated, and were then subjected to subcellular fractionation. The amounts of endogenous cytochrome *c* and α-tubulin (internal control) in the cytosolic fraction were determined by immunoblot analysis with specific antibodies. (**B**) COS-1 cells were transfected for 20 h with expression vectors for GFP, MKK7-JNK(WT) and either Bcl-XL, 14-3-3σ S186A or the corresponding WT proteins, as indicated. They were then stained with Hoechst 33342 (6.7 μg/ml) for 10 min, and the percentage of GFP-positive cells with pyknotic nuclei was determined. Data are means ± s.d. of values obtained from three fields of 200–300 cells in each of three independent experiments (*$P<0.0005$ and **$P<0.005$). (**C**) HeLa cells were incubated first for 30 min with or without 20 μM SP600125 and then for 3 h in the presence or absence of anisomycin (10 μg/ml). They were then stained with Hoechst 33342 (6.7 μg/ml) for 10 min, and the percentage of cells with pyknotic nuclei was determined. Data are means ± s.d. of values obtained from three fields of 100–200 cells in each of two independent experiments (*$P<0.0005$). (**D**) HeLa cells were transfected with expression vectors for GFP and JBD and then for 3 h in the presence or absence of anisomycin (10 μg/ml). They were then stained with Hoechst 33342 (6.7 μg/ml) for 10 min, and the percentage of GFP-positive cells with pyknotic nuclei was determined. Data are means ± s.d. of values obtained from three fields of 100–150 cells (*$P<0.0005$). (**E**) HeLa cells were transfected with expression vectors for GFP and either Bcl-XL, 14-3-3σ S186A or the corresponding WT protein, and then for 3 h in the presence or absence of anisomycin (10 μg/ml). They were then stained with Hoechst 33342 (6.7 μg/ml) for 10 min, and the percentage of GFP-positive cells with pyknotic nuclei was determined and shown as in (C) (*$P<0.0005$ and **$P<0.005$).

JNK activation (data not shown). Furthermore, anisomycin-induced phosphorylation of 14-3-3 proteins (14-3-3ζ and 14-3-3σ) was inhibited by pretreatment of cells with the JNK inhibitor SP600125 (Figure 4E), suggesting that JNK activation is required for anisomycin-induced 14-3-3 phosphorylation *in vivo*.

To further examine phosphorylation of 14-3-3 upon JNK activation *in vivo*, we carried out two-dimensional gel electrophoresis to separate hyper- and hypophosphorylated forms of 14-3-3. We detected two spots of 14-3-3σ in control (vector-transfected) HCT116 cells. Expression of MKK7-JNK(WT) (Figure 4F) or treatment with anisomycin (data not shown) resulted in a marked increase in the spot with greater negative charge (Spot 1) and a corresponding decrease in the other spot (Spot 2). We confirmed that Spot 1 is a phosphorylated form of Spot 2, as alkaline phosphatase treatment of MKK7-JNK(WT)-expressing cell extracts reduced Spot 1 and increased Spot 2 (data not shown). These results suggest that a high proportion of 14-3-3σ becomes phosphorylated upon JNK activation.

JNK promotes dissociation of Bax from 14-3-3 proteins

We next asked whether JNK-mediated phosphorylation of 14-3-3 affects the interaction between Bax and 14-3-3. Immunoprecipitation of 14-3-3σ from HCT116 cell lysates resulted in the co-precipitation of endogenous Bax (Figure 5A). Expression of MKK7-JNK(WT), but not that of MKK7-JNK(KN), resulted in a marked decrease in the amount of Bax that co-precipitated with 14-3-3σ. This effect of MKK7-JNK(WT) was not affected by coexpression of p35,

suggesting that JNK promotes the dissociation of Bax from 14-3-3 independently of caspase activation.

Exposure of HCT116 cells to anisomycin also reduced the amount of Bax that co-immunoprecipitated with 14-3-3σ (Figure 5B). Pretreatment of cells with the caspase inhibitor Z-VAD-CH_2DCB had no effect on the anisomycin-induced dissociation of Bax from 14-3-3, whereas pretreatment with the JNK inhibitor SP600125 blocked this effect of anisomycin. These results thus suggest that JNK mediates the anisomycin-induced dissociation of Bax from 14-3-3.

To examine further whether JNK-induced dissociation of Bax from 14-3-3 is dependent on the phosphorylation status of 14-3-3, we performed glutathione *S*-transferase (GST) pull-down assays with a GST–14-3-3ζ fusion protein (Figure 5C). Incubation of GST–14-3-3ζ, but not that of GST alone, with HeLa cell lysates resulted in the co-precipitation of Bax by glutathione-Sepharose. However, prior phosphorylation of GST-14-3-3ζ by MKK7–JNK(WT) led to a marked decrease (approximately 90% reduction) in the amount of Bax that co-precipitated with GST-14-3-3ζ. The S184A mutant of GST-14-3-3ζ precipitated similar amounts of Bax, regardless of whether or not it had been preincubated with MKK7–JNK(WT). These results are thus consistent with the notion that JNK-mediated phosphorylation of 14-3-3ζ at Ser184 reduces its affinity for Bax.

14-3-3 mutants inhibit Bax translocation, cytochrome c release and cell death

If 14-3-3 is a major target for JNK in induction of Bax translocation, one might expect that expression of a phosphorylation site mutant of 14-3-3 would block JNK-induced Bax translocation. Indeed, expression of either 14-3-3ζ S184A or 14-3-3σ S186A mutant inhibited MKK7–JNK- and anisomycin-induced GFP–Bax translocation to mitochondria (Figure 6A and B and Supplementary Figure 9). In addition, when distribution of endogenous Bax was assessed by subcellular fractionation, expression of 14-3-3ζ S184A mutant inhibited the increase of Bax protein in the mitochondrial fraction induced by MKK7–JNK (Supplementary Figure 10). Importantly, in both assays, 14-3-3 WT was less effective than its SA mutant in suppression of JNK-induced Bax translocation (Figure 6A and B and Supplementary Figure 10), suggesting strongly that phosphorylation of 14-3-3 at this Ser residue is critical for Bax translocation to mitochondria upon JNK activation.

We next examined whether 14-3-3 mutants inhibited JNK-induced cytochrome *c* release and cell death. The amount of endogenous cytochrome *c* detected in the cytosolic fraction was increased when MKK7–JNK(WT), but not MKK7–JNK(KN), was expressed in COS-1 cells (Figure 7A and data not shown). In contrast, co-expression of 14-3-3ζ S184A mutant, and that of the corresponding 14-3-3 WT to a lesser extent, inhibited MKK7–JNK (WT)-induced cytochrome *c* release, whereas the amount of the cytosolic marker α-tubulin in the cytosolic fraction was unaffected by MKK7–JNK or the 14-3-3 mutants (Figure 7A). Expression of MKK7–JNK (WT) in COS-1 cells induced chromatin condensation, an indication of cell death (Figure 7B). However, expression of 14-3-3σ SA mutant rendered the cells resistant to this effect of MKK7–JNK (WT) (Figure 7B). Moreover, 14-3-3σ WT was less effective in protecting cells from MKK7–JNK (WT)-induced cell death, compared to the 14-3-3σ SA mutant (Figure 7B). We next asked whether the 14-3-3σ mutant can inhibit anisomycin-induced cell death. Treatment of HeLa cells with anisomycin resulted in cell death, and pretreatment with SP600125 or coexpression of JBD or DN JNK partially blocked this effect (Figure 7C and D and Supplementary Figure 11), suggesting that JNK is required for anisomycin-induced cell death in HeLa cells. We found that expression of 14-3-3σ SA mutant blocked anisomycin-induced cell death, and 14-3-3σ WT was less effective compared to the 14-3-3σ SA mutant (Figure 7E), supporting the notion that phosphorylation of 14-3-3 by JNK plays an important role in JNK-mediated cell death.

Discussion

Recent studies have demonstrated that JNK plays a pivotal role in activation of the intrinsic apoptotic pathway that is mediated by mitochondria in response to cellular stress (Davis, 2000). Although Bax has been shown to be necessary for this action of JNK, the nature of the functional relation between these two proteins has been unclear. We now provide several lines of evidence that demonstrate that JNK-mediated phosphorylation of 14-3-3 induces the release of Bax from 14-3-3 and triggers its translocation to the mitochondria: (1) expression of an active form of JNK promoted Bax translocation to mitochondria; (2) inhibition of JNK (either by a chemical inhibitor or by a DN mutant) reduced the extent of Bax translocation to mitochondria in response to cellular stress; (3) JNK phosphorylated 14-3-3ζ at Ser-184 and 14-3-3σ at Ser-186 both *in vitro* and *in vivo*, and such phosphorylation reduced the affinity of 14-3-3 proteins for Bax; (4) expression of active JNK or treatment of cells with anisomycin induced the dissociation of Bax from 14-3-3 proteins; and (5) expression of phosphorylation site mutants of 14-3-3 proteins inhibited Bax translocation to mitochondria. These results strongly indicate that JNK regulates the activity of Bax by phosphorylating 14-3-3 proteins.

The initial studies of the role of JNK in apoptotic signals were performed by investigating neuronal cell death in response to neurotrophic factor withdrawal (Xia *et al*, 1995). The role for JNK in stress-induced neuronal cell death was confirmed by the studies of mice with a targeted disruption of the neuronal gene JNK3 (Yang *et al*, 1997). Although the JNK3 knockout mice are developmentally normal, they are resistant to excitotoxins. A similar resistance was observed in mice with a germ-line mutation in the c-Jun gene that replaced the JNK phosphorylation sites with alanine (Behrens *et al*, 1999). These data suggested that JNK mediates transcription-dependent apoptotic signals in neurons. In contrast, in non-neuronal cells, the JNK-mediated cytochrome *c* release and apoptosis induced by UV do not require *de novo* gene expression (Tournier *et al*, 2000). It is thus likely that relevant targets of JNK required for cytochrome *c* release and apoptosis are already present in these cells. Potential targets of JNK that may regulate cytochrome *c* release and apoptosis include members of the Bcl-2 family. The anti-apoptotic members Bcl-2, Bcl-x_L and Mcl-1, and the pro-apoptotic members Bad, Bim and Bmf are phosphorylated by JNK, although the significance of these phosphorylation events remains unclear (Ito *et al*, 1997; Maundrell *et al*, 1997; Kharbanda *et al*, 2000; Donovan *et al*, 2002; Inoshita *et al*, 2002; Lei and Davis, 2003; Putcha *et al*, 2003). We have

now shown that expression of phosphorylation site mutants of 14-3-3, and 14-3-3 WT to a lesser extent, suppressed JNK-induced Bax translocation, mitochondrial cytochrome *c* release and subsequent cell death. We confirmed that the 14-3-3 mutant did not hamper JNK-mediated phosphorylation of other targets such as c-Jun (F Tsuruta and Y Gotoh, unpublished results). These results strongly suggest that 14-3-3 protein is a major target of JNK in induction of these apoptotic events.

The JNK-mediated phosphorylation of 14-3-3β and 14-3-3ζ was found to occur at the previously identified phosphorylation sites (Aitken *et al*, 1995); 14-3-3β and 14-3-3ζ phosphorylated at these sites were named 14-3-3α and 14-3-3δ, respectively. It remains to be determined how such phosphorylation leads to the dissociation of Bax from 14-3-3. However, since the JNK phosphorylation sites reside within the domain responsible for the interaction of 14-3-3 with Bax (Nomura *et al*, 2003), it is likely that phosphorylation impairs the interaction at the binding interface. Alternatively, although the overall structure of 14-3-3 proteins is thought to be relatively rigid (Liu *et al*, 1995; Xiao *et al*, 1995), it is possible that phosphorylation might change the global conformation of 14-3-3 and thereby induce the dissociation of Bax.

On the Bax side, the 14-3-3-interacting domains are in the NH_2- and COOH-terminal regions (Nomura *et al*, 2003). Interestingly, previous studies have proposed that these regions are masked when Bax is in the inactive form and are exposed upon activation. Indeed, antibodies against certain epitopes at the NH_2-terminal region (cf. 6A7 monoclonal antibody) can react only with active Bax (Nechushtan *et al*, 1999; Lei *et al*, 2002). It is thus possible that 14-3-3 proteins physically conceal the NH_2- and COOH-terminal domains of Bax and thereby maintain it in its inactive form, and that dissociation of Bax from 14-3-3 may be essential for its activation in addition to the conformational change of Bax. According to this scenario, our observation that phosphorylation of 14-3-3 by JNK releases Bax from 14-3-3 may explain how JNK activates Bax. Consistent with this notion, targeted disruption of JNK genes has been shown to prevent the activation of Bax in response to cellular stresses, as judged by the lack of reactivity toward the 6A7 antibody (Lei *et al*, 2002).

Another proposed mechanism of Bax activation is a conformational change due to acidification or alkalization of the cytoplasmic pH (Khaled *et al*, 1999; Nomura *et al*, 2003). However, we could not detect a significant change in the signal level of a pH indicator incorporated into the cytoplasm in the presence or absence of activated JNK in our preliminary experiments (F Tsuruta and Y Gotoh, unpublished results), suggesting that it is unlikely that JNK promotes Bax activation indirectly through regulation of cytoplasmic pH.

Whereas we have shown that three 14-3-3 isoforms (β, ζ and σ) serve as JNK targets, some isoforms (γ, η and θ) do not possess a corresponding JNK phosphorylation site. One of these isoforms (θ) has been reported to be cleaved by caspase, resulting in dissociation of Bax (Nomura *et al*, 2003). Our results indicate that caspase activity is dispensable for the JNK-dependent dissociation of Bax from 14-3-3, indicating the existence of two independent mechanisms to regulate their dissociation. Since caspase is activated downstream of JNK, it is possible that phosphorylation-dependent release of Bax from 14-3-3 takes place first, and the caspase-dependent release of Bax subsequently amplifies the apoptotic signal through positive feedback.

Recently, it has been reported that Ku70 and Humanin also prevent apoptosis through sequestration of Bax (Guo *et al*, 2003; Sawada *et al*, 2003). However, Sawada *et al* (2003) have shown that the absence of Ku70 is not sufficient for inducing the apoptotic level of Bax translocation to mitochondria in the absence of apoptotic stimuli. Guo *et al* (2003) have also demonstrated that elimination of endogenous Humanin does not induce Bax translocation to mitochondria and apoptosis in healthy cells. It is thus likely that several cytoplasmic anchors for Bax work in parallel to sequester Bax from mitochondria, and dissociation of Bax from all or some of these cytoplasmic anchors may be required for initiation of Bax translocation to mitochondria.

In conclusion, we have demonstrated that JNK promotes Bax translocation to mitochondria through phosphorylation of 14-3-3 proteins. This finding may account at least in part for the apoptosis-inducing activity of the JNK and shed light on the mechanism of stress-induced apoptosis.

Materials and methods

The Materials and methods used in this study are described in Supplementary data.

Supplementary data

Supplementary data are available at *The EMBO Journal* Online.

Acknowledgements

We thank J Inagawa and K Ueda for technical supports with the two-dimensional gel electrophoresis, Drs R Dolmetsch and X Wang for critical reading of the manuscript, Drs M Miura, M Yaffe, H Fu, B Vogelstein and R Davis for providing reagents, and members of the Gotoh laboratory for helpful discussions and technical support.

References

Aitken A, Howell S, Jones D, Madrazo J, Patel Y (1995) 14-3-3 alpha and delta are the phosphorylated forms of raf-activating 14-3-3 beta and zeta. *In vivo* stoichiometric phosphorylation in brain at a Ser-Pro-Glu-Lys MOTIF. *J Biol Chem* **270:** 5706–5709

Behrens A, Sibilia M, Wagner EF (1999) Amino-terminal phosphorylation of c-Jun regulates stress-induced apoptosis and cellular proliferation. *Nat Genet* **21:** 326–329

Benton R, Palacios IM, Johnston DS (2002) Drosophila 14-3-3/PAR-5 is an essential mediator of PAR-1 function in axis formation. *Dev Cell* **3:** 659–671

Brunet A, Bonni A, Zigmond MJ, Lin MZ, Juo P, Hu LS, Anderson MJ, Arden KC, Blenis J, Greenberg ME (1999) Akt promotes cell survival by phosphorylating and inhibiting a Forkhead transcription factor. *Cell* **96:** 857–868

Datta SR, Dudek H, Tao X, Masters S, Fu H, Gotoh Y, Greenberg ME (1997) Akt phosphorylation of BAD couples survival signals to the cell-intrinsic death machinery. *Cell* **91:** 231–241

Davis RJ (2000) Signal transduction by the JNK group of MAP kinases. *Cell* **103:** 239–252

Dickens M, Rogers JS, Cavanagh J, Raitano A, Xia Z, Halpern JR, Greenberg ME, Sawyers CL, Davis RJ (1997) A cytoplasmic inhibitor of the JNK signal transduction pathway. *Science* **277:** 693–696

Donovan N, Becker EB, Konishi Y, Bonni A (2002) JNK phosphorylation and activation of BAD couples the stress-activated

signaling pathway to the cell death machinery. *J Biol Chem* **277:** 40944–40949

Du X, Fox JE, Pei S (1996) Identification of a binding sequence for the 14-3-3 protein within the cytoplasmic domain of the adhesion receptor, platelet glycoprotein Ib alpha. *J Biol Chem* **271:** 7362–7367

Gilmore AP, Metcalfe AD, Romer LH, Streuli CH (2000) Integrin-mediated survival signals regulate the apoptotic function of Bax through its conformation and subcellular localization. *J Cell Biol* **149:** 431–446

Gross A, McDonnell JM, Korsmeyer SJ (1999) BCL-2 family members and the mitochondria in apoptosis. *Genes Dev* **13:** 1899–1911

Guo B, Zhai D, Cabezas E, Welsh K, Nouraini S, Satterthwait AC, Reed JC (2003) Humanin peptide suppresses apoptosis by interfering with Bax activation. *Nature* **423:** 456–461

Harris CA, Johnson Jr EM (2001) BH3-only Bcl-2 family members are coordinately regulated by the JNK pathway and require Bax to induce apoptosis in neurons. *J Biol Chem* **276:** 37754–37760

Hsu YT, Wolter KG, Youle RJ (1997) Cytosol-to-membrane redistribution of Bax and Bcl-X(L) during apoptosis. *Proc Natl Acad Sci USA* **94:** 3668–3672

Inoshita S, Takeda K, Hatai T, Terada Y, Sano M, Hata J, Umezawa A, Ichijo H (2002) Phosphorylation and inactivation of myeloid cell leukemia 1 by JNK in response to oxidative stress. *J Biol Chem* **277:** 43730–43734

Ito T, Deng X, Carr B, May WS (1997) Bcl-2 phosphorylation required for anti-apoptosis function. *J Biol Chem* **272:** 11671–11673

Khaled AR, Kim K, Hofmeister R, Muegge K, Durum SK (1999) Withdrawal of IL-7 induces Bax translocation from cytosol to mitochondria through a rise in intracellular pH. *Proc Natl Acad Sci USA* **96:** 14476–14481

Kharbanda S, Saxena S, Yoshida K, Pandey P, Kaneki M, Wang Q, Cheng K, Chen YN, Campbell A, Sudha T, Yuan ZM, Narula J, Weichselbaum R, Nalin C, Kufe D (2000) Translocation of SAPK/JNK to mitochondria and interaction with Bcl-x(L) in response to DNA damage. *J Biol Chem* **275:** 322–327

Knudson CM, Tung KS, Tourtellotte WG, Brown GA, Korsmeyer SJ (1995) Bax-deficient mice with lymphoid hyperplasia and male germ cell death. *Science* **270:** 96–99

Krammer PH (2000) CD95's deadly mission in the immune system. *Nature* **407:** 789–795

Kuan CY, Yang DD, Samanta Roy DR, Davis RJ, Rakic P, Flavell RA (1999) The Jnk1 and Jnk2 protein kinases are required for regional specific apoptosis during early brain development. *Neuron* **22:** 667–676

Kuwana T, Mackey MR, Perkins G, Ellisman MH, Latterich M, Schneiter R, Green DR, Newmeyer DD (2002) Bid, Bax, and lipids cooperate to form supramolecular openings in the outer mitochondrial membrane. *Cell* **111:** 331–342

Lei K, Davis RJ (2003) JNK phosphorylation of Bim-related members of the Bcl2 family induces Bax-dependent apoptosis. *Proc Natl Acad Sci USA* **100:** 2432–2437

Lei K, Nimnual A, Zong WX, Kennedy NJ, Flavell RA, Thompson CB, Bar-Sagi D, Davis RJ (2002) The Bax subfamily of Bcl2-related proteins is essential for apoptotic signal transduction by c-Jun NH(2)-terminal kinase. *Mol Cell Biol* **22:** 4929–4942

Lindsten T, Ross AJ, King A, Zong WX, Rathmell JC, Shiels HA, Ulrich E, Waymire KG, Mahar P, Frauwirth K, Chen Y, Wei M, Eng VM, Adelman DM, Simon MC, Ma A, Golden JA, Evan G, Korsmeyer SJ, MacGregor GR, Thompson CB (2000) The combined functions of proapoptotic Bcl-2 family members bak and bax are essential for normal development of multiple tissues. *Mol Cell* **6:** 1389–1399

Liu D, Bienkowska J, Petosa C, Collier RJ, Fu H, Liddington R (1995) Crystal structure of the zeta isoform of the 14-3-3 protein. *Nature* **376:** 191–194

Masters SC, Pederson KJ, Zhang L, Barbieri JT, Fu H (1999) Interaction of 14-3-3 with a nonphosphorylated protein ligand, exoenzyme S of *Pseudomonas aeruginosa*. *Biochemistry* **38:** 5216–5221

Masuyama N, Oishi K, Mori Y, Ueno T, Takahama Y, Gotoh Y (2001) Akt inhibits the orphan nuclear receptor Nur77 and T-cell apoptosis. *J Biol Chem* **276:** 32799–32805

Maundrell K, Antonsson B, Magnenat E, Camps M, Muda M, Chabert C, Gillieron C, Boschert U, Vial-Knecht E, Martinou JC, Arkinstall S (1997) Bcl-2 undergoes phosphorylation by c-Jun N-terminal kinase/stress-activated protein kinases in the presence of the constitutively active GTP-binding protein Rac1. *J Biol Chem* **272:** 25238–25242

Molton SA, Todd DE, Cook SJ (2003) Selective activation of the c-Jun N-terminal kinase (JNK) pathway fails to elicit Bax activation or apoptosis unless the phosphoinositide 3′-kinase (PI3K) pathway is inhibited. *Oncogene* **22:** 4690–4701

Muslin AJ, Tanner JW, Allen PM, Shaw AS (1996) Interaction of 14-3-3 with signaling proteins is mediated by the recognition of phosphoserine. *Cell* **84:** 889–897

Nechushtan A, Smith CL, Hsu YT, Youle RJ (1999) Conformation of the Bax C-terminus regulates subcellular location and cell death. *EMBO J* **18:** 2330–2341

Nomura M, Shimizu S, Sugiyama T, Narita M, Ito T, Matsuda H, Tsujimoto Y (2003) 14-3-3 interacts directly with and negatively regulates pro-apoptotic Bax. *J Biol Chem* **278:** 2058–2065

Putcha GV, Deshmukh M, Johnson Jr EM (1999) BAX translocation is a critical event in neuronal apoptosis: regulation by neuroprotectants, BCL-2, and caspases. *J Neurosci* **19:** 7476–7485

Putcha GV, Le S, Frank S, Besirli CG, Clark K, Chu B, Alix S, Youle RJ, LaMarche A, Maroney AC, Johnson Jr EM (2003) JNK-mediated BIM phosphorylation potentiates BAX-dependent apoptosis. *Neuron* **38:** 899–914

Putcha GV, Moulder KL, Golden JP, Bouillet P, Adams JA, Strasser A, Johnson EM (2001) Induction of BIM, a proapoptotic BH3-only BCL-2 family member, is critical for neuronal apoptosis. *Neuron* **29:** 615–628

Sabapathy K, Kallunki T, David JP, Graef I, Karin M, Wagner EF (2001) c-Jun NH2-terminal kinase (JNK)1 and JNK2 have similar and stage-dependent roles in regulating T cell apoptosis and proliferation. *J Exp Med* **193:** 317–328

Saito M, Korsmeyer SJ, Schlesinger PH (2000) BAX-dependent transport of cytochrome *c* reconstituted in pure liposomes. *Nat Cell Biol* **2:** 553–555

Samuel T, Weber HO, Rauch P, Verdoodt B, Eppel JT, McShea A, Hermeking H, Funk JO (2001) The G2/M regulator 14-3-3sigma prevents apoptosis through sequestration of Bax. *J Biol Chem* **276:** 45201–45206

Sawada M, Sun W, Hayes P, Leskov K, Boothman DA, Matsuyama S (2003) Ku70 suppresses the apoptotic translocation of Bax to mitochondria. *Nat Cell Biol* **5:** 320–329

Shimizu S, Narita M, Tsujimoto Y (1999) Bcl-2 family proteins regulate the release of apoptogenic cytochrome *c* by the mitochondrial channel VDAC. *Nature* **399:** 483–487

Svennelid F, Olsson A, Piotrowski M, Rosenquist M, Ottman C, Larsson C, Oecking C, Sommarin M (1999) Phosphorylation of Thr-948 at the C terminus of the plasma membrane H(+)-ATPase creates a binding site for the regulatory 14-3-3 protein. *Plant Cell* **11:** 2379–2391

Tournier C, Hess P, Yang DD, Xu J, Turner TK, Nimnual A, Bar-Sagi D, Jones SN, Flavell RA, Davis RJ (2000) Requirement of JNK for stress-induced activation of the cytochrome *c*-mediated death pathway. *Science* **288:** 870–874

Tsujimoto Y, Shimizu S (2000) Bcl-2 family: life-or-death switch. *FEBS Lett* **466:** 6–10

Tsuruta F, Masuyama N, Gotoh Y (2002) The phosphatidylinositol 3-kinase (PI3K)-Akt pathway suppresses Bax translocation to mitochondria. *J Biol Chem* **277:** 14040–14047

van Hemert MJ, Steensma HY, van Heusden GP (2001) 14-3-3 proteins: key regulators of cell division, signalling and apoptosis. *BioEssays* **23:** 936–946

Wang X (2001) The expanding role of mitochondria in apoptosis. *Genes Dev* **15:** 2922–2933

Wei MC, Zong WX, Cheng EH, Lindsten T, Panoutsakopoulou V, Ross AJ, Roth KA, MacGregor GR, Thompson CB, Korsmeyer SJ (2001) Proapoptotic BAX and BAK: a requisite gateway to mitochondrial dysfunction and death. *Science* **292:** 727–730

Whitfield J, Neame SJ, Paquet L, Bernard O, Ham J (2001) Dominant-negative c-Jun promotes neuronal survival by reducing BIM expression and inhibiting mitochondrial cytochrome *c* release. *Neuron* **29:** 629–643

Wolter KG, Hsu YT, Smith CL, Nechushtan A, Xi XG, Youle RJ (1997) Movement of Bax from the cytosol to mitochondria during apoptosis. *J Cell Biol* **139:** 1281–1292

Xia Z, Dickens M, Raingeaud J, Davis RJ, Greenberg ME (1995) Opposing effects of ERK and JNK-p38 MAP kinases on apoptosis. *Science* **270:** 1326–1331

Xiao B, Smerdon SJ, Jones DH, Dodson GG, Soneji Y, Aitken A, Gamblin SJ (1995) Structure of a 14-3-3 protein and implications for coordination of multiple signalling pathways. *Nature* **376:** 188–191

Yaffe MB (2002) How do 14-3-3 proteins work? Gatekeeper phosphorylation and the molecular anvil hypothesis. *FEBS Lett* **513:** 53–57

Yaffe MB, Rittinger K, Volinia S, Caron PR, Aitken A, Leffers H, Gamblin SJ, Smerdon SJ, Cantley LC (1997) The structural basis for 14-3-3:phosphopeptide binding specificity. *Cell* **91:** 961–971

Yamaguchi H, Wang HG (2001) The protein kinase PKB/Akt regulates cell survival and apoptosis by inhibiting Bax conformational change. *Oncogene* **20:** 7779–7786

Yang DD, Kuan CY, Whitmarsh AJ, Rincon M, Zheng TS, Davis RJ, Rakic P, Flavell RA (1997) Absence of excitotoxicity-induced apoptosis in the hippocampus of mice lacking the Jnk3 gene. *Nature* **389:** 865–870

Yuan J, Yankner BA (2000) Apoptosis in the nervous system. *Nature* **407:** 802–809

Zha J, Harada H, Yang E, Jockel J, Korsmeyer SJ (1996) Serine phosphorylation of death agonist BAD in response to survival factor results in binding to 14-3-3 not BCL-X(L). *Cell* **87:** 619–628

Zhang L, Chen J, Fu H (1999) Suppression of apoptosis signal-regulating kinase 1-induced cell death by 14-3-3 proteins. *Proc Natl Acad Sci USA* **96:** 8511–8515

Zong WX, Lindsten T, Ross AJ, MacGregor GR, Thompson CB (2001) BH3-only proteins that bind pro-survival Bcl-2 family members fail to induce apoptosis in the absence of Bax and Bak. *Genes Dev* **15:** 1481–1486

Involvement of caspase-4 in endoplasmic reticulum stress-induced apoptosis and Aβ-induced cell death

Junichi Hitomi,[1,6] Taiichi Katayama,[1,6] Yutaka Eguchi,[2,6,7] Takashi Kudo,[3] Manabu Taniguchi,[1,6] Yoshihisa Koyama,[1,6] Takayuki Manabe,[1,6] Satoru Yamagishi,[1,6] Yoshio Bando,[4] Kazunori Imaizumi,[5] Yoshihide Tsujimoto,[2,6,7] and Masaya Tohyama[1,6]

[1]Department of Anatomy and Neuroscience, [2]Division of Molecular Genetics, and [3]Division of Psychiatry and Behavioural Proteomics, Department of Post-Genomics and Diseases, Graduate School of Medicine, Osaka University, Suita, Osaka 565-0871, Japan
[4]Department of Anatomy, Asahikawa Medical College, Midorigaoka Higashi, Asahikawa, Hokkaido, 078-8510, Japan
[5]Division of Structural Cell Biology, Nara Institute of Science and Technology, Takayama, Ikoma, Nara 630-0101, Japan
[6]21st Century COE Program, Japan Society for the Promotion of Science, Chiyoda-ku, Tokyo 102-8471, Japan
[7]Solution Oriented Research for Science and Technology of Japan, Science and Technology Agency, Honcho 4-1-8, Kawaguchi, Saitama, 332-0012, Japan

Recent studies have suggested that neuronal death in Alzheimer's disease or ischemia could arise from dysfunction of the endoplasmic reticulum (ER). Although caspase-12 has been implicated in ER stress-induced apoptosis and amyloid-β (Aβ)–induced apoptosis in rodents, it is controversial whether similar mechanisms operate in humans. We found that human caspase-4, a member of caspase-1 subfamily that includes caspase-12, is localized to the ER membrane, and is cleaved when cells are treated with ER stress-inducing reagents, but not with other apoptotic reagents. Cleavage of caspase-4 is not affected by overexpression of Bcl-2, which prevents signal transduction on the mitochondria, suggesting that caspase-4 is primarily activated in ER stress-induced apoptosis. Furthermore, a reduction of caspase-4 expression by small interfering RNA decreases ER stress-induced apoptosis in some cell lines, but not other ER stress-independent apoptosis. Caspase-4 is also cleaved by administration of Aβ, and Aβ-induced apoptosis is reduced by small interfering RNAs to caspase-4. Thus, caspase-4 can function as an ER stress-specific caspase in humans, and may be involved in pathogenesis of Alzheimer's disease.

Introduction

Recently, it has been reported that some human diseases, such as Alzheimer's disease (AD), Parkinson's diseases, and cystic fibrosis, and neuronal damage by ischemia are related to stress acting on the ER, which leads to intraluminal accumulation of unfolded proteins (Katayama et al., 1999; Wigley et al., 1999; Imai et al., 2000, 2001; Nakagawa et al., 2000; Sato et al., 2001; Tamatani et al., 2001). Stress on the ER can be induced in vitro by depletion of calcium from the ER lumen, inhibition of asparagine N-linked glycosylation, reduction of disulfide bonds, expression of mutant proteins, and ischemia (Imaizumi et al., 2001). ER stress induces three major cellular responses: unfolded protein response (UPR), ER-associated degradation, and apoptosis. Cells exposed to ER stress can up-regulate genes encoding chaperones that facilitate the protein folding process in the ER and reduce overall translation (UPR; Harding et al., 1999; Kaufman, 2002; Forman et al., 2003), or enhance proteasomal degradation of misfolded ER protein in cytosol (Bonifacino and Weissman, 1998; Travers et al., 2000), to reduce the accumulation and aggregation of misfolded proteins, and relieve cells from the stress (Kozutsumi et al., 1988). On the other hand, excessive or long-termed ER stress results in apoptotic cell death, involving nuclear fragmentation,

Address correspondence to Taiichi Katayama, Dept. of Anatomy and Neuroscience, Graduate School of Medicine, Osaka University, Suita, Osaka 565-0871, Japan. Tel.: 81-6-6879-3221. Fax: 81-6-6879-3229. email: katayama@anat2.med.osaka-u.ac.jp; or Yutaka Eguchi, Division of Molecular Genetics, Dept. of Post-Genomics and Disease, Graduate School of Medicine, Osaka University, Suita, Osaka 565-0871, Japan. Tel.: 81-6-6879-3363. Fax: 81-6-6879-3369.
email: eguchi@gene.med.osaka-u.ac.jp

Key words: apoptosis; ER stress; caspase-4; Alzheimer's disease; amyloid-β

Abbreviations used in this paper: Aβ, amyloid-β; AD, Alzheimer's disease; ICE, interleukin-1β converting enzyme; RNAi, RNA interference; siRNA, small interfering RNA; TRAF2, tumor necrosis factor receptor–associated factor 2; UPR, unfolded protein response.

The Journal of Cell Biology, Volume 165, Number 3, May 10, 2004 347–356
http://www.jcb.org/cgi/doi/10.1083/jcb.200310015

condensation of chromatin, and shrinkage of the cell body (Imaizumi et al., 2001). Several mechanisms that activate apoptotic signaling pathways have been reported. For example, the UPR increases the transcription of CHOP/GADD153 (Brewer et al., 1997), which is closely associated with cell death (Zinszner et al., 1998), recruitment of tumor necrosis factor receptor–associated factor 2 (TRAF2) to activated IRE1α induces c-Jun NH_2-terminal kinase activation (Urano et al., 2000), or calpain activates downstream caspase cascade (Nakagawa and Yuan, 2000). However, little is known about the precise mechanisms to lead to ER stress-induced cell death in humans.

Activation of caspases, a family of cysteine proteases that cleave substrates at specific aspartate residues, is a central mechanism in the apoptotic cell death process (Salvesen and Dixit, 1997; Thornberry and Lazebnik, 1998). Most of apoptosis-inducing stimuli lead to release of cytochrome *c* from mitochondria, which binds to Apaf-1 to activate caspase-9 (Li et al., 1997; Zou et al., 1997), one of initiator caspases with a long pro-domain, and then the activated caspase-9 cleaves effector caspases (Li et al., 1997), including caspases 3 and 7 with a relatively short pro-domain, to activate them. Antiapoptotic Bcl-2 family proteins can rescue cells from apoptosis by protecting mitochondria to prevent cytochrome *c* release (Kluck et al., 1997; Yang et al., 1997). Several initiator caspases are known to be activated upstream of the mitochondrial dysfunction by specific apoptotic stimuli. For example, Fas stimulation can activate caspase-8 (Fernandes-Alnemri et al., 1996; Muzio et al., 1996), which cannot be inhibited by Bcl-2 (Scaffidi et al., 1998). Among 14 known caspases, caspase-12 seems to be involved in signaling pathways specific to ER stress-induced apoptosis (Nakagawa et al., 2000). Pro–caspase-12 is predominantly localized to the ER, and is specifically cleaved by ER stress. Furthermore, caspase-12–deficient mice show a reduced sensitivity to amyloid-β (Aβ), which is found in brains from Alzheimer's patients (Selkoe, 1986) and shown to cause neuronal cytotoxicity (Yankner et al., 1989). Based on these findings, caspase-12 has been suggested to play an important role in the pathogenesis of AD and to represent a potential target of treatment. However, caspase-12 has only been cloned in the mouse and rat so far, and therefore it is controversial whether similar mechanisms operate in humans (Katayama et al., 1999; Rao et al., 2001; Fischer et al., 2002).

Human genome sequence that is highly homologous to mouse caspase-12 has been identified at the locus within the caspase-1/interleukin-1β converting enzyme (ICE) genes cluster on chromosome 11q22.3 (Fischer et al., 2002), but the gene is interrupted by frame shift and premature stop codon, and also has amino acid substitution in the critical site for caspase activity (Fischer et al., 2002). Therefore, human caspase-12 seems to be lost, and the caspases that substitute for caspase-12 to be activated specifically by ER stress have not been identified in humans so far. We described here that human caspase-4 located within the caspase-1/ICE genes cluster shows similar characteristics to mouse caspase-12. The role of the caspase-4 in ER stress-induced apoptosis and Aβ-induced cell death will be discussed.

Results

Identification of caspase-4 as a gene homologous to caspase-12

To detect a caspase that was specifically involved in ER stress, we screened human colon cDNA libraries by the plaque hybridization method using the mouse caspase-12 gene as a probe. Human caspase-4 was cloned as the most homologous gene to mouse caspase-12, in agreement with the fact that both molecules belong to the caspase-1/ICE subfamily within the caspase family (Kamens et al., 1995; Lin et al., 2000). Although caspase-5, which has slightly less homology to caspase-12 (caspase-4: 48%; caspase-5: 45%), was also isolated, the screening process yielded much more caspase-4 clones than caspase-5. Because caspase-4 but not caspase-5 was expressed in the cell lines used in this work, which underwent apoptosis in response to ER stress, we assumed that human caspase-4 might functionally substitute for mouse caspase-12 in the human system, and further analyzed the possible role of caspase-4 as a mediator of ER stress-induced apoptosis.

Subcellular localization of caspase-4

First, we studied the subcellular localization of endogenous caspase-4 in SK-N-SH human neuroblastoma cells. Immunofluorescence microscopy showed that immunostaining pattern of caspase-4 strictly overlapped with that of ER markers such as GRP78 and GRP94 (Fig. 1, a–c). Immunoreactivity of caspase-4 was found to overlap only in part with fluorescence signals from Mitotracker (Fig. 1, d–f). These results suggest that caspase-4 was localized predominantly to the ER, and to the mitochondria in addition. The similar results were obtained using HeLa cells (Fig. 1, g–l). When caspase-4 fused with GFP at its COOH terminus was overexpressed in HeLa cells to see the subcellular localization in live cells, most of the fluorescent signals from caspase-4/GFP fusion protein overlapped with those from ER-tracker (Fig. 1, m–o), confirming predominant localization of caspase-4 to the ER by non-immunological method. The immunoelectron microscopic analysis showed that the immunoreactive signals for caspase-4 were found on the ER and mitochondria (Fig. 1, p–r), but much less signals on the nuclei (Fig. 1 r). We also performed biochemical fractionation analysis. Although we could not eliminate contamination of ER marker proteins in the mitochondria-enriched fraction using SK-N-SH cells, probably because we could not disrupt cells homogeneously as the cell line displays heterogeneity in cellular morphology, microsome-enriched fraction does not seem to contain mitochondria and cytosol (Fig. 1 s). Under these conditions, caspase-4 was recovered in both mitochondria-enriched fraction and microsome-enriched fraction, and in cytosolic fraction to a lesser extent (Fig. 1 s), indicating that caspase-4 was surely in microsome-enriched fraction. From these results, we concluded that caspase-4 was localized to the ER, and to the mitochondria in addition, in both SK-N-SH and HeLa cells.

Specific cleavage of caspase-4 by ER stress and Aβ treatments

To examine whether caspase-4 was specifically cleaved by ER stress, we analyzed the cleavage of pro–caspase-4 in re-

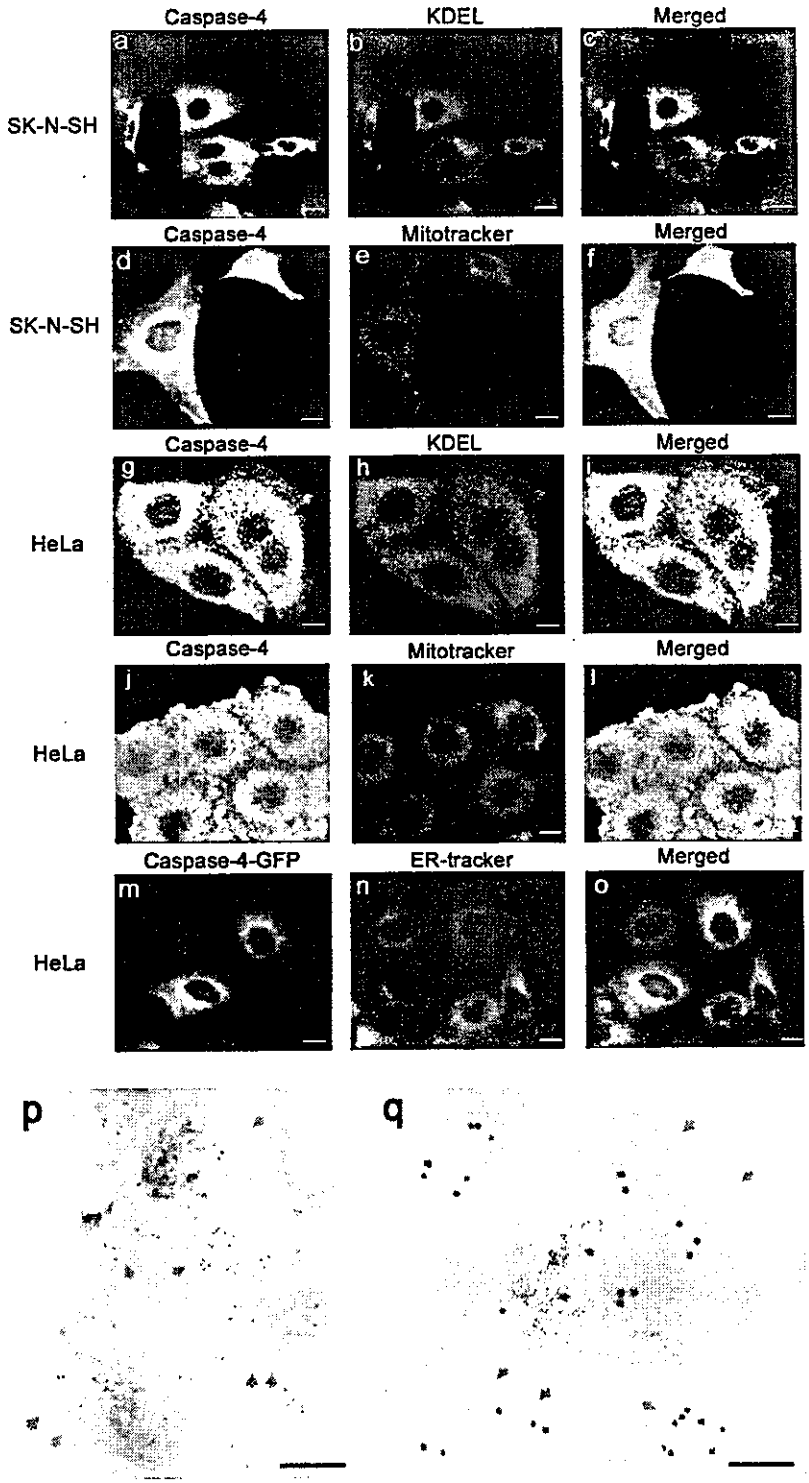

r

	Nuclear	Mitochondria	ER	Cytosol	total
Gold	0	359	392	169	920
%	0	39	43	18	100

s

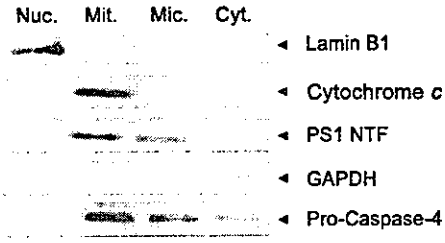

Figure 1. **Localization of caspase-4 in SK-N-SH and HeLa cells.** (a–l) SK-N-SH cells (a–f) or HeLa cells (g–l) were stained with anti–caspase-4 and anti-KDEL antibodies (a and g, caspase-4, green; b and h, KDEL, red; c and i, overlapping, yellow), or with anti–caspase-4 antibody and Mitotracker (d and j, caspase-4, green; e and k, Mitotracker, red; f and l, overlapping, yellow), and observed under a confocal microscope as described in Materials and methods. Anti-KDEL antibody detects both GRP78 and GRP94 (ER markers), whereas Mitotracker stains the mitochondria. (m–o) HeLa cells were transfected with a caspase-4–GFP fusion gene, and were stained with ER-tracker (m, caspase-4, green; n, ER-tracker, blue; o, overlapping, blue-green), and observed under a nonconfocal fluorescence microscope. Bars, 5 μm. (p and q) Immunoelectron microscopic analysis was performed for SK-N-SH cells as described in Materials and methods. Photograph shown in panel q is the enlarged image of a part of photograph p. Gold grains showed the immunoreactivity of caspase-4, and blue and red arrows showed the ER and mitochondria, respectively. Bars: (p) 200 nm; (q) 90 nm. (r) Gold grains observed on indicated organelles in immunoelectron microscopic analysis were counted and displayed. (s) Biochemical fractionation was performed as described in Materials and methods, and analyzed by Western blotting using the indicated antibodies. Lamin B1, nuclear marker; cytochrome c, mitochondrial marker; presenilin-1 NH_2-terminal fragment (PS1 NTF), microsomal marker; and glyceraldehyde-3-phosphate dehydrogenase (GAPDH), cytosolic marker.

sponse to several apoptotic stimuli (Fig. 2 a). We found that cleavage of pro–caspase-4 was induced in SK-N-SH cells by treatment with tunicamycin and thapsigargin, both of which caused ER stress. In contrast, when cells were exposed to non-ER stress inducers such as etoposide, staurosporine, and UV at a dose providing similar extent of cell death to that by tunicamycin and thapsigargin, final cleavage products of pro–caspase-4 (Fig. 2 a, cleaved-caspase-4, arrowhead) was not observed. Although the bands shown by the asterisks in Fig. 2 a, which should be derived from pro–caspase-4 by unknown processing reaction, judging from the data below (Fig. 4 b), were also increased, they were also observed in nontreated cells, so we speculated that the bands were not the final processed form of caspase-4. Under the same conditions, cleavage of caspases 3 and 7, the downstream caspases, was observed regardless of apoptotic stimulations (Fig. 2 a). These results suggest that caspase-4 is specifically activated by apoptotic stimuli inducing ER stress, but not by other stimuli that do not cause ER stress.

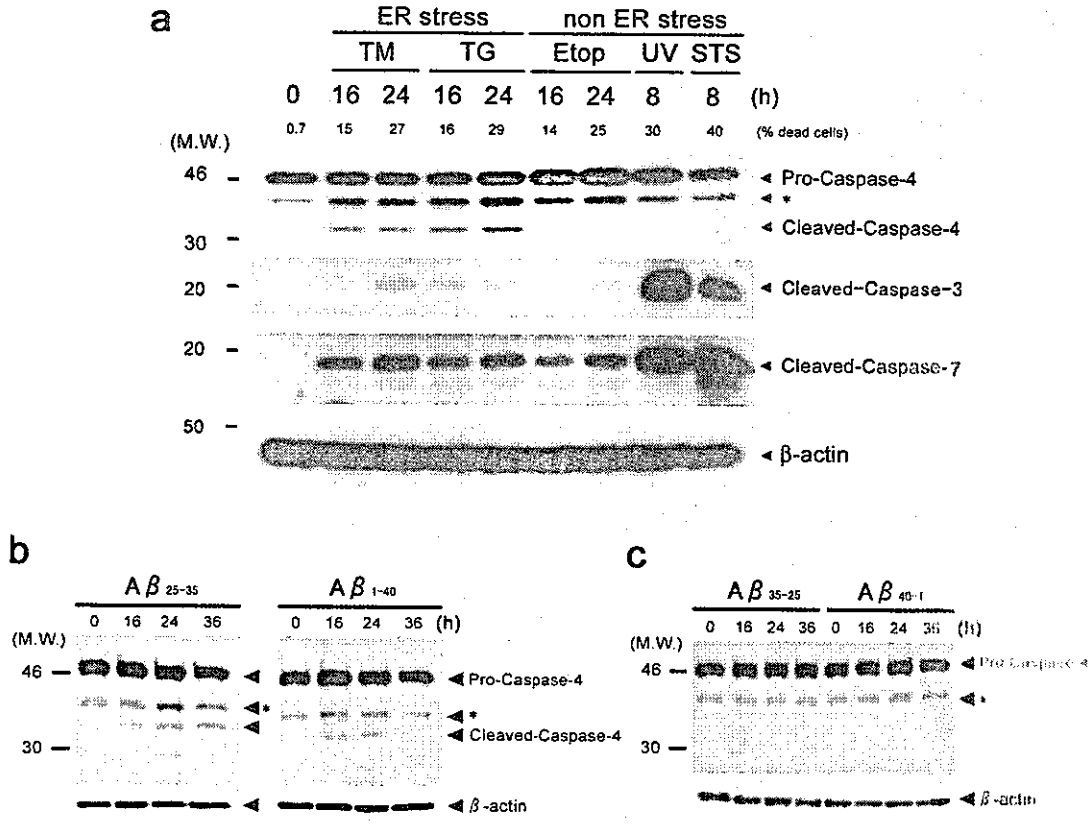

Figure 2. **Specific cleavage of caspase-4 by ER stress and Aβ treatment.** (a) SK-N-SH cells were treated with 1 μg/ml tunicamycin (TM), 0.5 μM thapsigargin (TG), 100 μM etoposide (Etop), or 0.1 μM staurosporine (STS) for indicated periods, or irradiated with 150 J/m^2 UV followed by incubation for indicated periods. Equal amounts of cell lysates (15 μg) were analyzed by Western blotting using anti–caspase-4 antibody (top), anti–caspase-3 antibody (second from top), anti–caspase-7 antibody (third from top), or anti–β-actin antibody (bottom). Positions of pro–caspase-4, cleaved caspase-4, cleaved caspase-3, cleaved caspase-7, and β-actin are indicated. Extent of cell death assessed by MTS assay after incubation for indicated periods are also shown at the top of the gels. (b) SK-N-SH cells were treated with 25 μM synthetic $A\beta_{25\text{-}35}$ or 5 μM $A\beta_{1\text{-}40}$ peptides for the indicated periods. Equal amounts of cell lysates (15 μg) were analyzed by Western blotting using anti–caspase-4 antibody (top) and anti–β-actin antibody (bottom) as a control. Positions of pro–caspase-4, cleaved caspase-4, and β-actin are indicated. (c) SK-N-SH cells were treated with the reverse peptides (25 μM $A\beta_{35\text{-}25}$ and 5 μM $A\beta_{40\text{-}1}$, respectively) for the indicated periods, and cleavage of caspase-4 was examined as in panel b. (a–c) Bands marked by asterisks are likely to be derived from pro–caspase-4 by unknown processing reaction.

To address the possibility that caspase-4 contributes to the mechanism of Aβ-induced cell death in humans, we examined the cleavage of caspase-4 in SK-N-SH cells after treatment with Aβ. When cells were incubated with 25 μM $A\beta_{25\text{-}35}$ or 5 μM $A\beta_{1\text{-}40}$, cleavage of caspase-4 was observed (Fig. 2 b). In contrast, treatment of cells with the reverse peptides ($A\beta_{35\text{-}25}$ and $A\beta_{40\text{-}1}$, respectively), which were not toxic, did not induce the cleavage of caspase-4 (Fig. 2 c). These results suggest that caspase-4 is activated by neurotoxic Aβ treatment similar to ER stress-induced apoptosis.

Cleavage of caspase-4 in the presence of Bcl-2

To confirm that cleavage of caspase-4 was not due to other caspases activated downstream of the mitochondrial pathway, we examined the effect of overexpression of Bcl-2 and Bcl-x_L on apoptosis induced by tunicamycin. Apoptotic nuclear morphological changes were induced by treatment of vector transfectants of SK-N-SH and of HeLa cells with tunicamycin for 30 h, but such changes were completely suppressed by overexpression of Bcl-2 (Fig. 3) or Bcl-x_L (not depicted), indicating that the apoptotic signaling pathway downstream of mitochondria was not operating in cells with overexpression of these antiapoptotic proteins. However, cleavage of caspase-4 after 16 h of tunicamycin treatment was only slightly affected by overexpression of Bcl-2 (Fig. 3) or Bcl-x_L (not depicted). These results suggested that caspase-4 is largely activated before the activation of effector caspases during ER stress-induced cell death.

Requirement of caspase-4 for ER stress- and Aβ-induced apoptosis

To determine whether caspase-4 is required for ER stress-induced cell death, SK-N-SH cells that expressed endogenous caspase-4 were transfected with small interfering RNA (siRNA) to caspase-4 or GFP as a control. Immunofluorescence analysis showed that the amount of caspase-4 was substantially decreased by incubation for 60 h after transfection with siRNA directed against caspase-4, but immunoreactivity of caspase-4 was not affected by transfection with GFP-siRNA, when compared with nontransfected cells (Fig. 4 a). Western blot analysis also showed that the amount of caspase-4 was decreased by siRNA to caspase-4 (Fig. 4 b). These re-

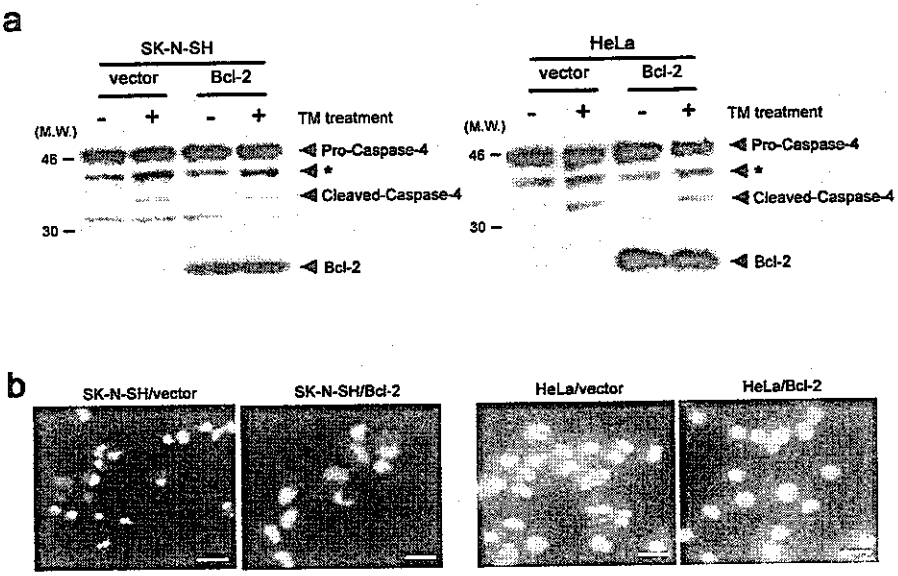

Figure 3. **No effect of Bcl-2 overexpression on ER stress-induced cleavage of caspase-4.** (a) SK-N-SH cells (left) and HeLa cells (right) stably transfected with the vector or a Bcl-2 expression system were incubated with (+) or without (−) 1 μg/ml tunicamycin for 16 h. Equal amounts of cell lysates were analyzed by Western blotting using anti–caspase-4 antibody (top) and anti–Bcl-2 antibody (bottom). Positions of pro–caspase-4, cleaved caspase-4, and Bcl-2 are indicated. Asterisks show processed caspase-4 as described in Fig. 2 a. (b) The indicated cells were treated with 1 μg/ml tunicamycin for 30 h, stained with Hoechst 33342, and observed under a fluorescence microscope. Bars, 25 μm.

sults showed that the siRNA could diminish the amount of caspase-4, and that the antibody used here specifically recognized caspase-4 in immunohistochemical analysis.

We next examined the effect of decrease in caspase-4 level by siRNA on ER stress-induced apoptosis. Assessment of cell death on the basis of morphological changes showed that ~60% of untransfected SK-N-SH cells were killed by treatment with thapsigargin for 40 h. The extent of cell death was unaffected by transfection with siRNA to GFP (Fig. 4 c). In contrast, only ~30% of the cells died after being transfected with caspase-4 siRNA and exposed to the same stimulation with thapsigargin (Fig. 4 c). As shown in Fig. 4 b, treatment with thapsigargin for 24 h yielded lower level of cleaved-caspase-4 in the cells transfected with caspase-4 siRNA than in the cells transfected with GFP-siRNA. Because the amount of cleaved caspase-4 shown in Fig. 4 b seemed to correlate with the extent of cell death in Fig. 4 c, incomplete inhibition of cell death by transfection with caspase-4 siRNA could be due to residual activity of caspase-4. These results indicate that cells with decreased expression of caspase-4 become more resistant to ER stress-induced cell death.

When cell death was examined by the MTS assay, treatment with caspase-4 siRNA, but not with GFP-siRNA, increased the resistance to ER stress-induced cell death (Fig. 4 d). The increase in the resistance to ER stress-induced cell death was also observed when siRNA to caspase-4 with a different sequence (caspase-4 siRNA-b) was used (Fig. 4 d), indicating that the effect was due to the decreased expression of caspase-4, but not by a specific side effect of caspase-4 siRNA that might affect the expression of other genes. On the other hand, the efficiency of cell death induced by etoposide treatment was not significantly affected by both caspase-4 siRNAs (Fig. 4 d). Therefore, caspase-4 is likely to be specifically involved in ER stress-induced cell death.

To know whether caspase-4 is involved in ER stress-induced cell death in other cell lines, we examined the effect of caspase-4 siRNA using HeLa cells. As shown in Fig. 4 e, treatment of HeLa cells with caspase-4 siRNA significantly increased the resistance to ER stress-induced cell death, although the extent of the increase in resistance was less than that observed for SK-N-SH cells. This is probably because some other apoptotic mechanisms might also operate simultaneously in HeLa cells. Therefore, we concluded that caspase-4 is likely to be involved in ER stress-induced cell death at least in part in HeLa cells.

We next examined whether caspase-4 is involved in Aβ-induced cell death. When treated with $A\beta_{25\text{-}35}$, SK-N-SH cells transfected with caspase-4 siRNA showed significant reduction in cell death compared with the cells transfected with GFP-siRNA (Fig. 4 f). From these results presented here, we concluded that caspase-4 is involved in Aβ-induced cell death, as well as in ER stress-induced cell death.

Discussion

It has been known that apoptotic morphological changes are observed in cell death caused by ER stress (Imaizumi et al., 2001). Caspases are activated to transmit apoptotic signals transcending the difference in species (Alnemri et al., 1996). In rodents, caspase-12 mediates apoptosis specifically in response to ER stress (Nakagawa et al., 2000). Although human caspase-12 gene is transcribed into mRNA, mature caspase-12 protein would not be produced, because the gene is interrupted by frame shift and premature stop codon (Fischer et al., 2002). Furthermore, it contains amino acid substitution in the critical site, which leads to loss of function in several caspases (Fischer et al., 2002). Thus, human caspase-12 does not seem to function in ER stress-induced apoptosis, and some other caspases with similar structure might substitute functionally for caspase-12 in humans. The caspase-12 gene is located within a region where caspase-1/ICE subfamily genes cluster (caspases 1, 4, 5, 12 in human and caspases 1, 11, 12 in mouse). No locus with a comparably high homology to rodent caspase-12 could be found in the human genome. Caspases 4 and 5 are located between caspases 1 and 12 in human genome, whereas only caspase-11 is located between caspases 1 and 12 in mouse. Although it is not known why the region in human genome contains gene duplication, caspases 4 and 5 have been thought to function similarly to caspases 11 and 12. Mouse caspase-11

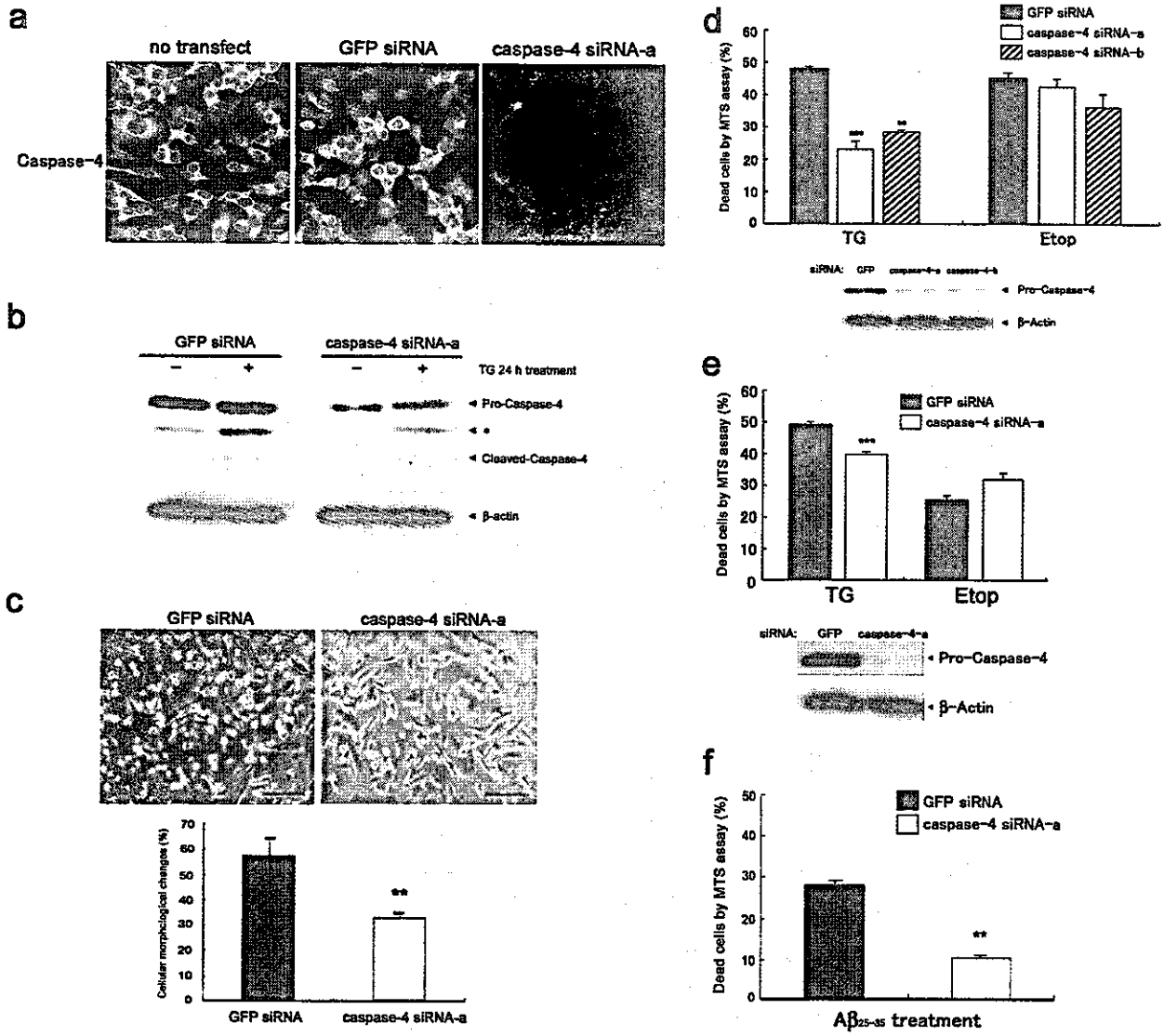

Figure 4. **Decrease in ER stress- or Aβ-induced cell death after siRNA-mediated reduction of caspase-4 expression.** (a) SK-N-SH cells were transfected with siRNA oligos (1 μg oligo/24 well plate) to GFP (control) or caspase-4 (siRNA-a). After incubation for 60 h, cells were fixed and stained with caspase-4 antibodies as described in Materials and methods. Bars, 5 μm. (b) Cells were transfected as in panel a. After incubation for 60 h, cells were incubated with (+) or without (−) 0.5 μM thapsigargin for 24 h. Equal amounts of cell lysates (10 μg) were analyzed by Western blotting using anti–caspase-4 antibody (top) or anti–β-actin antibody (bottom). (c) Top panels show representative phase-contrast images of GFP siRNA-transfected cells (left) and caspase-4 siRNA-a–transfected cells (right) after treatment with 0.5 μM thapsigargin for 40 h. The bottom panel shows the extent of cell death assessed by morphological changes, and expressed as the mean ± SEM for three independent experiments as described in Materials and methods. Asterisks show a significant difference from controls (GFP siRNA-transfected cells): **, indicates $P < 0.01$. Bars, 50 μm. (d) Cells were transfected with the indicated siRNAs, and cell viability after 0.5 μM thapsigargin or 100 μM etoposide treatment for 40 h was estimated by the MTS assay. Results were expressed as the mean ± SEM for three independent experiments. Asterisks show a significant difference from controls: **, indicates $P < 0.01$; ***, indicates $P < 0.001$. Bottom panel shows reduction of caspase-4 level by the indicated siRNAs assessed by Western blotting as described in panel b. (e) HeLa cells were transfected with GFP siRNA or caspase-4 siRNA-a as described in Materials and methods. After incubation for 24 h, cells were incubated with 0.5 μM thapsigargin for 40 h, and then viability was estimated as described in panel d. Each value represents the mean ± SEM for three independent experiments. Asterisks show a significant difference from controls: ***, indicates $P < 0.001$. (f) SK-N-SH cells were transfected with GFP siRNA or caspase-4 siRNA-a. After incubation for 60 h, cells were incubated with 25 μM $A\beta_{25\text{-}35}$ peptide for 40 h, and then viability was estimated as described in panel d. Each value represents the mean ± SEM for three independent experiments. Asterisks show a significant difference from controls: **, indicates $P < 0.01$.

is essential for the activation of caspase-1/ICE to promote pro–IL-1β (interleukin-1β) processing (Wang et al., 1996, 1998). On the other hand, caspase-5 is likely involved in processing of pro–IL-1β together with caspase-1/ICE (Martinon et al., 2002) and the caspase-5 gene resembles the mouse caspase-11 in its lipopolysaccharide inducibility (Lin et al., 2000). Therefore, caspase-5 should be the orthologue of caspase-11. Here, the screening process yielded the caspase-4 gene as the homologous gene to mouse caspase-12. Thus, caspase-4 is the best candidate that would function similarly to mouse caspase-12 in ER stress-induced cell death in humans.

Here, we examined the localization of human caspase-4 using several methods. The immunostaining analysis using anti–caspase-4 antibody and fluorescent analysis for caspase-4/GFP fusion protein in Fig. 1 showed the predominant localization of caspase-4 on the ER. On the other hand, the immuno-EM showed the nearly equal distribution of caspase-4 on the ER and mitochondria, and subcellular fractionation showed that caspase-4 was recovered in the microsome-enriched and mitochondria-enriched fractions, and also in cytosolic fraction. Although we could not eliminate contamination of ER marker proteins in the mitochondria-enriched fraction in subcellular fractionation using SK-N-SH cells, microsome-enriched fraction does not seem to contain mitochondria and cytosol. Under these conditions, caspase-4 was recovered in both mitochondria-enriched fraction and microsome-enriched fraction, and amounts of caspase-4 recovered in the microsome-enriched and mitochondria-enriched fractions were comparable to those of ER marker, presenilin-1. Therefore, considering all the results shown in Fig. 1, we concluded that caspase-4 was localized to the ER membrane, and probably to the mitochondria in addition.

Caspase-4 on the ER is supposed to function in ER stress-induced apoptosis similarly to caspase-12. In supporting this hypothesis, caspase-4 was cleaved specifically by ER stress and Aβ-treatment, but not by other apoptotic stimuli including etoposide, staurosporine, and UV. Additionally because Bcl-2 that can completely inhibit the signaling pathway at least downstream from mitochondria, did not prevent the cleavage of caspase-4 by ER stress, it should be most probable that caspase-4 on the ER but not on mitochondria is primarily cleaved. We also showed that reduction of the level of caspase-4 by RNA interference (RNAi) resulted in decrease in ER stress-induced cell death and Aβ-induced cell death, but did not affect cell death induced by etoposide. The characteristics of human caspase-4 shown here are very similar to those of mouse caspase-12 reported previously (Nakagawa et al., 2000), and therefore, caspase-4 is able to substitute the caspase-12 functions in ER stress-induced apoptosis and Aβ-induced cell death. Because caspase-4 was also localized to the mitochondria in addition to the ER membrane, whereas caspase-12 was shown to localize predominantly to the ER, but not to the mitochondria (Nakagawa et al., 2000), caspase-4 might have additional function compared with caspase-12, although the function of caspase-4 on mitochondria is not clear.

Several mechanisms that activate caspase-12 have been proposed in mouse system. For example, calpain, a protease that can be activated by calcium released from ER upon ER stress, starts cleavage of caspase-12 (Nakagawa and Yuan, 2000), caspase-7 activates caspase-12 upon prolonged ER stress (Rao et al., 2001), or TRAF2 mediates caspase-12 activation, which is regulated by IRE1α (Yoneda et al., 2001). It is not clear which mechanism is involved in activation of caspase-4, but because final cleavage products were not observed in cells with activated caspase-7 (Fig. 2 a), activation of caspase-7 does not seem to be enough for full activation of caspase-4. To know the precise mechanism that activate caspase-4, it should be important to find proteins that interact with pro–caspase-4 during ER stress-induced apoptosis.

The inhibition of apoptosis induced by ER stress exposure by RNAi to caspase-4 was incomplete. It is possible that the residual activity of caspase-4 after RNAi would be responsible for the cell death. Alternatively, other apoptotic mechanisms might also operate simultaneously. Several possible pathways have been postulated for ER stress-induced apoptosis. ER stress is reported to activate ASK–c-Jun NH_2-terminal kinase pathway through the IRE1–TRAF2–ASK1 complex formation (Nishitoh et al., 2002). Other signaling pathway is mediated by transcriptional activation of genes encoding proapoptotic function. Activation of stress transducer IRE1, PERK, or ATF6 leads to transcriptional activation of CHOP/GADD153, a bZIP transcription factor that potentiates apoptosis (Oyadomari et al., 2002). Operation of these mechanisms might account for incomplete inhibition of ER stress-induced apoptosis by knockout of caspase-12 and knockdown of caspase-4 in mouse and humans, respectively. It is possible that caspase-dependent mechanism and other mechanisms function in parallel in initiating ER stress-induced apoptosis, and the mechanism that mainly operates could differ depending on cell types. We have shown that the extent to decrease in cell death by decreasing caspase-4 level of SK-N-SH cells was comparable to that reported for caspase-12 knockout mouse (Nakagawa et al., 2000), whereas that of HeLa cells was relatively less. We also find some cells, like HUVEC, in which decrease in caspase-4 did not affect the ER stress-induced apoptosis (unpublished data). Thus, caspase-4 has been shown to function in ER stress-induced apoptosis at least in several cell lines, including SK-N-SH and HeLa cells, but not all cells.

Cell death caused by Aβ treatment was also partially inhibited by RNAi to caspase-4. Although it is controversial whether Aβ-induced cell death involves ER stress-induced apoptosis, the results are consistent that these two types of cell death are mediated by common mechanism at least in part. Recent report described that the cell death induced by Aβ was inhibited by the broad-spectrum caspase inhibitor z-VAD and more specifically by the down-regulation of caspase-2 with antisense oligonucleotides (Haviv et al., 1998). Neuronal culture derived from caspase-2 null mice was also shown to be partially resistant to $A\beta_{1\text{-}42}$ toxicity (Troy et al., 2000). Thus $A\beta_{1\text{-}42}$-induced cell death might be mediated by caspase-2 as well as caspase-12. It is possible that both caspases 2 and 4 are involved in Aβ-induced cell death also in the human system.

Because caspase-4 seems to be responsible for cell death after Aβ treatment, caspase-4 might be involved in pathogenesis of AD. Consistently to this hypothesis, our preliminary analysis showed an increase in cytoplasmic staining for caspase-4 in the pyramidal cell layer of the hippocampal CA1-2 region in AD patients, but not in control brains (unpublished data). All of the AD brains tested had stronger caspase-4 immunoreactivity than disease control brains from patients with other neurodegenerative disorders ($n = 4$ for AD and $n = 3$ for disease control), and the strong staining was remarkable in the pyramidal neurons around deposits of β-amyloid. Increased caspase-4 might elevate the vulnerability of neurons to apoptosis, and therefore may be involved in the pathogenesis of AD.

Bcl-2 family proteins play essential roles in regulating apoptosis. Although antiapoptotic family members (Bcl-2, Bcl-x_L) and multidomain proapoptotic members (Bak, Bax) are thought to function mainly on mitochondria, recent studies suggest that they may also function on the ER where they reside as well. Overexpression of Bcl-2 (Foyouzi-Youssefi et al., 2000; Pinton et al., 2000) or knockout of both Bak and Bax (Scorrano et al., 2003) are reported to reduce ER Ca^{2+} concentration, but other reports showed that Bcl-2 enhanced the retention of Ca^{2+} in the ER lumen (Distelhorst et al., 1996; He et al., 1997). Thus, although it is still controversial, Bcl-2 family members may contribute to regulating ER stress-induced apoptosis on the ER (Ferri and Kroemer, 2001; Scorrano et al., 2003; Zong et al., 2003) in addition to their main function on mitochondria. Our results demonstrate that overexpressed Bcl-2 and Bcl-x_L, which can completely inhibit the signaling pathway at least downstream from mitochondria, did not prevent, but slightly affected, the cleavage of caspase-4 by ER stress. The slight decrease might be due to the absence of its feed back cleavage by downstream effector caspases, such as caspase-3. Therefore, without regard to the mitochondria or the ER where Bcl-2 family functions, activation of caspase-4 should be the primary reaction in ER stress-induced activation of caspases.

In this work, we discovered that caspase-4 plays a key role in ER stress-induced apoptosis in humans. Caspase-4 also seems to act in the β-amyloid–induced cell death, suggesting that human caspase-4 corresponds to rodent caspase-12 to initiate cell death signaling pathway, and that the activation of caspase-4 would mediate neuronal cell death in neurodegenerative disorder. Caspase-4 could be the potential target to develop treatments for such diseases including AD.

Materials and methods

Chemicals and antibodies

We used the following antibodies: anti–caspase-4 mAb (4B9; MBL International Corporation), anti–caspase-4 pAb (Santa Cruz Biotechnology, Inc.), anti-KDEL mAb (10C3; StressGen Biotechnologies), anti–Lamin B1 mAb (L-5; Zymed Laboratories), anti–cytochrome *c* mAb (7H8.2C12; BD Biosciences), anti–glyceraldehyde-3-phosphate dehydrogenase mAb (6G7; Biogenesis), anti–caspase-3 mAb (19; Transduction), anti–caspase-7 mAb (4G2; MBL International Corporation), anti–β-actin mAb (C4; CHEMICON International Inc.), anti–Bcl-2 mAb (#100; BD Biosciences), Alexa 588–conjugated anti–mouse IgG antibody (Molecular Probes), FITC-conjugated anti–goat IgG antibody (Jackson ImmunoResearch Laboratories), gold-conjugated anti–goat IgG antibody (British BioCell), and HRP-conjugated anti–mouse IgG antibody (Cell Signaling). Anti–presenilin-1 polyclonal antibody was raised by immunizing rabbits with a synthetic peptide corresponding to residues 1–14 of human presenilin-1, and was affinity purified using ProtOn Kit1 (MultiplePeptide Systems). The chemical reagents used in this experiment were tunicamycin, thapsigargin, etoposide, staurosporine (Sigma-Aldrich), and ER-tracker and Mitotracker (Molecular Probes). Cytotoxic peptides, $A\beta_{25-35}$ and $A\beta_{1-40}$, and their reverse peptides, $A\beta_{35-25}$ and $A\beta_{40-1}$, were purchased from Sigma-Aldrich.

Cell culture

Human neuroblastoma SK-N-SH cells and human carcinoma HeLa cells were respectively cultured in α-MEM (Invitrogen) and DME (Invitrogen) both containing 10% FBS, at 37°C under 5% CO_2. For some experiments, these cells were stably transfected with pCAGGS-hBcl-2 (Iwahashi et al., 1997) and pCAGGS-hBcl-x_L (Tagami et al., 2000) to overexpress Bcl-2 and Bcl-x_L, respectively.

cDNA cloning

A human colon cDNA library (Stratagene) was used for hybridization to isolated cDNA homologous to the partial sequence of mouse caspase-12 gene.

Immunofluorescence microscopy

SK-N-SH cells or HeLa cells were incubated with or without Mitotracker probes, and were fixed with 0.1 M phosphate buffer containing 4% PFA for 2 h at 4°C. Cells were incubated with anti–caspase-4 pAb with or without anti-KDEL mAb, followed by FITC- and Alexa 588–conjugated secondary antibodies, respectively. Stained cells were observed under a confocal microscope (model LSM510; Carl Zeiss MicroImaging, Inc.). To determine localization of caspase-4 in live cells, HeLa cells were transfected with caspase-4/GFP fusion gene subcloned into a pcDNA3.1 (Invitrogen) to produce caspase-4 fused with GFP at its COOH terminus, and after 24 h, cells were incubated with ER-tracker probe for 30 min, followed by observation under a fluorescence microscope (model IX71; Olympus).

Immuno-EM

Immuno-EM was performed essentially as described previously (Miyake et al., 2002). In brief, SK-N-SH cells cultured on a 15-cm dish were fixed with 4% PFA in PBS, pH 7.2, at RT for several hours. After harvesting the cells, they were washed with 30 mM Hepes buffer, pH 7.4, several times. The cells were resuspended in 10% gelatin in 30 mM Hepes buffer, pH 7.4, at 37°C. After centrifugation to recover cells, gelatin was solidified on ice. Blocks for ultracryotomy were prepared and infused with 20% polyvinylpyrrolidone/1.84 M sucrose overnight at 4°C. Ultrathin sections were collected on nickel grids and immunostained with anti–caspase-4 pAb. The sections were incubated with gold-conjugated anti–goat IgG antibody (gold particles, 10-nm diam) for 1 h at RT. Grids were contracted in 2% uranyl acetate and examined on a transmission electron microscope (model CM10; Philips).

Subcellular fractionation

SK-N-SH cells cultured on a 15-cm dish were washed twice with PBS, harvested, and suspended in buffer A (50 mM Tris-HCl, pH 8.0, 1 mM EDTA, 0.32 M sucrose, 0.1 mM PMSF) for 5 min on ice. Then the cells were passed through a 25-gauge needle 13 times and centrifuged at 500 *g* for 10 min to collect a crude nuclear pellet. The supernatant was centrifuged at 1,200 *g* for 10 min to yield a mitochondria-enriched pellet, which contained mitochondria and microsome as shown in Fig. 1 s. This supernatant was further centrifuged at 100,000 *g* for 60 min to yield a microsomal pellet and a cytosolic fraction. All of the pellets were dissolved in buffer A containing 1% SDS. Equal volume of each fraction was subjected to Western blotting as described below, using indicated antibodies.

Western blot analysis

Cells treated with the indicated reagents were washed with PBS, harvested, and lysed in TNE buffer (10 mM Tris-HCl, pH 7.8, 1 mM EDTA, 150 mM NaCl, 1 mM PMSF) containing 0.5% NP-40. Equal amounts of protein were subjected to 12% SDS-PAGE and transferred to a PVDF membrane (Millipore). The membrane was blocked with 5% BSA and was incubated with each primary antibody, followed by incubation with an HRP-conjugated secondary antibody. Proteins were visualized with an ECL detection system (Amersham Biosciences).

Preparation and transfection of siRNAs

The annealed double-stranded siRNAs listed below were obtained from Dharmacon, and were used to decrease expression of caspase-4. Caspase-4 siRNA-a: 5′-AAGUGGCCUCUUCACAGUCAUdTdT-3′ (sense), 5′-AAAUGACUGUGAAGAGGCCACdTdT-3′ (antisense); caspase-4 siRNA-b: 5′-AAGAUUUCCUCACUGGUGUUUdTdT-3′ (sense), 5′-AAAAACACCAGTGAGGAAATCdTdT-3′ (antisense). For control, siRNA to GFP was used. GFP siRNA: 5′-P-GGCUACGUCCAGGAGCGCACC-3′ (sense), 5′-P-UGCGCUCCUGGACGUAGCCUU-3′ (antisense). These sequences were not significantly homologous to genes other than caspase-4 or GFP by BLAST search (NCBI). SK-N-SH cells were transfected at 50% confluence in 24-well plastic plates with 1.0 μg of each of the above siRNAs using Transmessenger transfection reagent (QIAGEN) according to the manufacturer's protocol. Transfected cells were incubated at 37°C for 60 h without changing the medium. siRNAs were introduced into HeLa cells by electroporation three times with 48-h intervals using Amaxa system according to the manufacturer's protocol. Efficiency of RNAi was measured by immunocytochemical analysis and Western blot analysis using anti–caspase-4 antibody or anti–β-actin antibody.

Cell viability assay

SK-N-SH cells or HeLa cells overexpressing Bcl-2 and Bcl-x_L, or transfected with siRNAs as above were treated with various reagents as indicated. When using $A\beta_{1-40}$, it was preincubated for 1 wk at 37°C to establish its cytotoxicity. Cell death was assessed on the basis of cellular morpho-

logical changes observed by phase-contrast microscopy or from nuclear morphological changes detected by fluorescence microscopy after staining the cells with 10 μM Hoechst 33342. At least 500 cells were counted, and the data was expressed as the mean ± SEM from three independent experiments and P values were calculated by *t* test. The MTS ([3-(4, 5-dimethylthiazol-2-yl)-5-(3-carboxymethoxyphenyl)-2-(4-sulfophenyl)-2H-tetrazolium, inner salt]) assay was also performed to evaluate cell viability. After treatment with apoptosis-inducing reagents, cells were coincubated with MTS solution (Promega) for 1 h at 37°C. The amount of reduced MTS released from the viable cells was quantified by measuring the absorbance at 490 nm using a spectrophotometer. Results were expressed as a ratio (%) of dead cells after treatments to those in control as above.

The authors greatly thank Ms. A. Arakawa and Ms. M. Matsumoto-Yatera for their technical assistance. We are grateful to Drs. J. Yuan, H. Ichijo, H. Nishitoh, S. Miyake, and M. Takeda for critical reading of the manuscript and for valuable advice and encouragement.

Submitted: 3 October 2003
Accepted: 6 April 2004

References

Alnemri, E.S., D.J. Livingston, D.W. Nicholson, G. Salvesen, N.A. Thornberry, W.W. Wong, and J. Yuan. 1996. Human ICE/CED-3 protease nomenclature. *Cell.* 87:171.

Bonifacino, J.S., and A.M. Weissman. 1998. Ubiquitin and the control of protein fate in the secretory and endocytic pathways. *Annu. Rev. Cell Dev. Biol.* 14: 19–57.

Brewer, J.W., J.L. Cleveland, and L.M. Hendershot. 1997. A pathway distinct from the mammalian unfolded protein response regulates expression of endoplasmic reticulum chaperones in non-stressed cells. *EMBO J.* 16:7207–7216.

Distelhorst, C.W., M. Lam, and T.S. McCormick. 1996. Bcl-2 inhibits hydrogen peroxide-induced ER Ca^{2+} pool depletion. *Oncogene.* 12:2051–2055.

Fernandes-Alnemri, T., R.C. Armstrong, J. Krebs, S.M. Srinivasula, L. Wang, F. Bullrich, L.C. Fritz, J.A. Trapani, K.J. Tomaselli, G. Litwack, and E.S. Alnemri. 1996. In vitro activation of CPP32 and Mch3 by Mch4, a novel human apoptotic cysteine protease containing two FADD-like domains. *Proc. Natl. Acad. Sci. USA.* 93:7464–7469.

Ferri, K.F., and G. Kroemer. 2001. Organelle-specific initiation of cell death pathways. *Nat. Cell Biol.* 3:E255–E263.

Fischer, H., U. Koenig, L. Eckhart, and E. Tschachler. 2002. Human caspase 12 has acquired deleterious mutations. *Biochem. Biophys. Res. Commun.* 293: 722–772.

Forman, M.S., V.M. Lee, and J.Q. Trojanowski. 2003. 'Unfolding' pathways in neurodegenerative disease. *Trends Neurosci.* 26:407–410.

Foyouzi-Youssefi, R., S. Arnaudeau, C. Borner, W.L. Kelley, J. Tschopp, D.P. Lew, N. Demaurex, and K.H. Krause. 2000. Bcl-2 decreases the free Ca^{2+} concentration within the endoplasmic reticulum. *Proc. Natl. Acad. Sci. USA.* 97:5723–5728.

Harding, H.P., Y. Zhang, and D. Ron. 1999. Protein translation and folding are coupled by an endoplasmic-reticulum-resident kinase. *Nature.* 397:271–274.

Haviv, R., L. Lindenboim, J. Yuan, and R. Stein. 1998. Need for caspase-2 in apoptosis of growth-factor-deprived PC12 cells. *J. Neurosci. Res.* 52:491–497.

He, H., M. Lam, T.S. McCormick, and C.W. Distelhorst. 1997. Maintenance of calcium homeostasis in the endoplasmic reticulum by Bcl-2. *J. Cell Biol.* 138:1219–1228.

Imai, Y., M. Soda, and R. Takahashi. 2000. Parkin suppresses unfolded protein stress-induced cell death through its E3 ubiquitin-protein ligase activity. *J. Biol. Chem.* 275:35661–35664.

Imai, Y., M. Soda, H. Inoue, N. Hattori, Y. Mizuno, and R. Takahashi. 2001. An unfolded putative transmembrane polypeptide, which can lead to endoplasmic reticulum stress, is a substrate of Parkin. *Cell.* 105:891–902.

Imaizumi, K., K. Miyoshi, T. Katayama, T. Yoneda, M. Taniguchi, T. Kudo, and M. Tohyama. 2001. The unfolded protein response and Alzheimer's disease. *Biochim. Biophys. Acta.* 1536:85–96.

Iwahashi, H., Y. Eguchi, N. Yasuhara, T. Hanafusa, Y. Matsuzawa, and Y. Tsujimoto. 1997. Synergistic anti-apoptotic activity between Bcl-2 and SMN implicated in spinal muscular atrophy. *Nature.* 390:413–417.

Kamens, J., M. Paskind, M. Hugunin, R.V. Talanian, H. Allen, D. Banach, N. Bump, M. Hackett, C.G. Johnston, P. Li, et al. 1995. Identification and characterization of ICH-2, a novel member of the interleukin-1 beta-converting enzyme family of cysteine proteases. *J. Biol. Chem.* 270:15250–15256.

Katayama, T., K. Imaizumi, N. Sato, K. Miyoshi, T. Kudo, J. Hitomi, T. Morihara, T. Yoneda, F. Gomi, Y. Mori, et al. 1999. Presenilin-1 mutations downregulate the signaling pathway of the unfolded-protein response. *Nat. Cell Biol.* 1:479–485.

Kaufman, R.J. 2002. Orchestrating the unfolded protein response in health and disease. *J. Clin. Invest.* 110:1389–1398.

Kluck, R.M., E. Bossy-Wetzel, D.R. Green, and D.D. Newmeyer. 1997. The release of cytochrome *c* from mitochondria: a primary site for Bcl-2 regulation of apoptosis. *Science.* 275:1132–1136.

Kozutsumi, Y., M. Segal, K. Normington, M.J. Gething, and J. Sambrook. 1988. The presence of malfolded proteins in the endoplasmic reticulum signals the induction of glucose-regulated proteins. *Nature.* 332:462–464.

Li, P., D. Nijhawan, I. Budihardjo, S.M. Srinivasula, M. Ahmad, E.S. Alnemri, and X. Wang. 1997. Cytochrome *c* and dATP-dependent formation of Apaf-1/caspase-9 complex initiates an apoptotic protease cascade. *Cell.* 91: 479–489.

Lin, X.Y., M.S. Choi, and A.G. Porter. 2000. Expression analysis of the human caspase-1 subfamily reveals specific regulation of the CASP5 gene by lipopolysaccharide and interferon-gamma. *J. Biol. Chem.* 275:39920–39926.

Martinon, F., K. Burns, and J. Tschopp. 2002. The inflammasome: a molecular platform triggering activation of inflammatory caspases and processing of proIL-beta. *Mol. Cell.* 10:417–426.

Miyake, S., T. Yamashita, M. Taniguchi, M. Tamatani, K. Sato, and M. Tohyama. 2002. Identification and characterization of a novel mitochondrial tricarboxylate carrier. *Biochem. Biophys. Res. Commun.* 295:463–468.

Muzio, M., A.M. Chinnaiyan, F.C. Kischkel, K. O'Rourke, A. Shevchenko, J. Ni, C. Scaffidi, J.D. Bretz, M. Zhang, R. Gentz, et al. 1996. FLICE, a novel FADD-homologous ICE/CED-3-like protease, is recruited to the CD95 (Fas/APO-1) death-inducing signaling complex. *Cell.* 85:817–827.

Nakagawa, T., and J. Yuan. 2000. Cross-talk between two cysteine protease families. Activation of caspase-12 by calpain in apoptosis. *J. Cell Biol.* 150:887–894.

Nakagawa, T., H. Zhu, N. Morishima, E. Li, J. Xu, B.A. Yankner, and J. Yuan. 2000. Caspase-12 mediates endoplasmic-reticulum-specific apoptosis and cytotoxicity by amyloid-beta. *Nature.* 403:98–103.

Nishitoh, H., A. Matsuzawa, K. Tobiume, K. Saegusa, K. Takeda, K. Inoue, S. Hori, A. Kakizuka, and H. Ichijo. 2002. ASK1 is essential for endoplasmic reticulum stress-induced neuronal cell death triggered by expanded polyglutamine repeats. *Genes Dev.* 16:1345–1355.

Oyadomari, S., E. Araki, and M. Mori. 2002. Endoplasmic reticulum stress-mediated apoptosis in pancreatic beta-cells. *Apoptosis.* 7:335–345.

Pinton, P., D. Ferrari, P. Magalhaes, K. Schulze-Osthoff, F. Di Virgilio, T. Pozzan, and R. Rizzuto. 2000. Reduced loading of intracellular $Ca^{(2+)}$ stores and downregulation of capacitative $Ca^{(2+)}$ influx in Bcl-2–overexpressing cells. *J. Cell Biol.* 148:857–862.

Rao, R.V., E. Hermel, S. Castro-Obregon, G. del Rio, L.M. Ellerby, H.M. Ellerby, and D.E. Bredesen. 2001. Coupling endoplasmic reticulum stress to the cell death program. Mechanism of caspase activation. *J. Biol. Chem.* 276:33869–33874.

Salvesen, G.S., and V.M. Dixit. 1997. Caspases: intracellular signaling by proteolysis. *Cell.* 91:443–446.

Sato, N., K. Imaizumi, T. Manabe, M. Taniguchi, J. Hitomi, T. Katayama, T. Yoneda, T. Morihara, Y. Yasuda, T. Takagi, et al. 2001. Increased production of beta-amyloid and vulnerability to endoplasmic reticulum stress by an aberrant spliced form of presenilin 2. *J. Biol. Chem.* 276:2108–2114.

Scaffidi, C., S. Fulda, A. Srinivasan, C. Friesen, F. Li, K.J. Tomaselli, K.M. Debatin, P.H. Krammer, and M.E. Peter. 1998. Two CD95 (APO-1/Fas) signaling pathways. *EMBO J.* 17:1675–1687.

Scorrano, L., S.A. Oakes, J.T. Opferman, E.H. Cheng, M.D. Sorcinelli, T. Pozzan, and S.J. Korsmeyer. 2003. BAX and BAK regulation of endoplasmic reticulum Ca^{2+}: a control point for apoptosis. *Science.* 300:135–139.

Selkoe, D.J. 1986. Altered structural proteins in plaques and tangles: what do they tell us about the biology of Alzheimer's disease? *Neurobiol. Aging.* 7:425–432.

Tagami, S., Y. Eguchi, M. Kinoshita, M. Takeda, and Y. Tsujimoto. 2000. A novel protein, RTN-XS, interacts with both Bcl-XL and Bcl-2 on endoplasmic reticulum and reduces their anti-apoptotic activity. *Oncogene.* 19:5736–5746.

Tamatani, M., T. Matsuyama, A. Yamaguchi, N. Mitsuda, Y. Tsukamoto, M. Taniguchi, Y.H. Che, K. Ozawa, O. Hori, H. Nishimura, et al. 2001. ORP150 protects against hypoxia/ischemia-induced neuronal death. *Nat. Med.* 7:317–323.

Thornberry, N.A., and Y. Lazebnik. 1998. Caspases: enemies within. *Science.* 281: 1312–1316.

Travers, K.J., C.K. Patil, L. Wodicka, D.J. Lockhart, J.S. Weissman, and P. Walter. 2000. Functional and genomic analyses reveal an essential coordina-

tion between the unfolded protein response and ER-associated degradation. *Cell.* 101:249–258.

Troy, C.M., S.A. Rabacchi, W.J. Friedman, T.F. Frappier, K. Brown, and M.L. Shelanski. 2000. Caspase-2 mediates neuronal cell death induced by beta-amyloid. *J. Neurosci.* 20:1386–1392.

Urano, F., X. Wang, A. Bertolotti, Y. Zhang, P. Chung, H.P. Harding, and D. Ron. 2000. Coupling of stress in the ER to activation of JNK protein kinases by transmembrane protein kinase IRE1. *Science.* 287:664–666.

Wang, S., M. Miura, Z. Jung, H. Zhu, V. Gagliardini, L. Shi, A.H. Greenberg, and J. Yuan. 1996. Identification and characterization of Ich-3, a member of the interleukin-1beta converting enzyme (ICE)/Ced-3 family and an upstream regulator of ICE. *J. Biol. Chem.* 271:20580–20587.

Wang, S., M. Miura, Y.K. Jung, H. Zhu, E. Li, and J. Yuan. 1998. Murine caspase-11, an ICE-interacting protease, is essential for the activation of ICE. *Cell.* 92:501–509.

Wigley, W.C., R.P. Fabunmi, M.G. Lee, C.R. Marino, S. Muallem, G.N. DeMartino, and P.J. Thomas. 1999. Dynamic association of proteasomal machinery with the centrosome. *J. Cell Biol.* 145:481–490.

Yang, J., X. Liu, K. Bhalla, C.N. Kim, A.M. Ibrado, J. Cai, T.I. Peng, D.P. Jones, and X. Wang. 1997. Prevention of apoptosis by Bcl-2: release of cytochrome *c* from mitochondria blocked. *Science.* 275:1129–1132.

Yankner, B.A., L.R. Dawes, S. Fisher, L. Villa-Komaroff, M.L. Oster-Granite, and R.L. Neve. 1989. Neurotoxicity of a fragment of the amyloid precursor associated with Alzheimer's disease. *Science.* 245:417–420.

Yoneda, T., K. Imaizumi, K. Oono, D. Yui, F. Gomi, T. Katayama, and M. Tohyama. 2001. Activation of caspase-12, an endoplastic reticulum (ER) resident caspase, through tumor necrosis factor receptor-associated factor 2-dependent mechanism in response to the ER stress. *J. Biol. Chem.* 276:13935–13940.

Zinszner, H., M. Kuroda, X. Wang, N. Batchvarova, R.T. Lightfoot, H. Remotti, J.L. Stevens, and D. Ron. 1998. CHOP is implicated in programmed cell death in response to impaired function of the endoplasmic reticulum. *Genes Dev.* 12:982–995.

Zong, W.X., C. Li, G. Hatzivassiliou, T. Lindsten, Q.C. Yu, J. Yuan, and C.B. Thompson. 2003. Bax and Bak can localize to the endoplasmic reticulum to initiate apoptosis. *J. Cell Biol.* 162:59–69.

Zou, H., W.J. Henzel, X. Liu, A. Lutschg, and X. Wang. 1997. Apaf-1, a human protein homologous to *C. elegans* CED-4, participates in cytochrome *c*-dependent activation of caspase-3. *Cell.* 90:405–413.

THE JOURNAL OF BIOLOGICAL CHEMISTRY
Vol. 279, No. 32, Issue of August 6, pp. 33865–33874, 2004
Printed in U.S.A.

A Caspase-8-independent Signaling Pathway Activated by Fas Ligation Leads to Exposure of the Bak N Terminus*

Received for publication, March 30, 2004, and in revised form, May 11, 2004
Published, JBC Papers in Press, May 24, 2004, DOI 10.1074/jbc.M403499200

Lilin Zhang‡, Shigeomi Shimizu‡, Kazuhiro Sakamaki§, Shin Yonehara§, and Yoshihide Tsujimoto‡¶

From the ‡Laboratory of Molecular Genetics, Department of Post-Genomics and Diseases, Osaka University Medical School and Solution-Oriented Research for Science and Technology, Japan Science and Technology Corp., 2-2 Yamadaoka, Suita, Osaka 565-0871 and the §Graduate School of Biostudies and Institute for Virus Research, Kyoto University, Kawahara-cho, Shogoin, Sakyo-ku, Kyoto 606-8507, Japan

Bak is a pro-apoptotic member of the Bcl-2 family that is activated by apoptotic stimulation: its activation is characterized by conformational changes such as exposure of the N terminus and oligomerization. In death receptor-mediated apoptosis, the activation of Bak depends on activation of caspase-8. However, we found that exposure of the N terminus of Bak (but not oligomerization) can occur in the absence of active caspase-8. Although exposure of the N terminus of Bak without oligomerization is not sufficient to release cytochrome *c* from the mitochondria and commit cells to apoptosis, this change sensitizes the mitochondria to apoptotic signals (including Bid) and thus sensitizes cells to apoptotic death. Fas-induced, caspase-8-independent exposure of the N terminus of Bak is blocked by staurosporine, a pan protein kinase inhibitor. These results suggest that Fas stimulation not only activates caspase-8, but also a distinct signaling pathway involving protein kinase(s) to induce exposure of the N terminus of Bak.

Mitochondria play a crucial role in many physiological and pathological cell death paradigms in mammals. Most apoptotic stimuli convey death signals to the mitochondria. During apoptosis, the permeability of the outer mitochondrial membrane increases, resulting in the release of proteins into the cytoplasm from the intermembrane space, including several apoptogenic molecules such as cytochrome *c*, Smac (Diablo), HtrA2 (Omi), and apoptosis-inducing factor. After being released into the cytoplasm, cytochrome *c* binds to apoptotic protease activating factor 1, which recruits and activates procaspase-9, triggering the activation of the caspase cascade and committing the cell to apoptotic death. Smac (Diablo) and HtrA2 (Omi) facilitate caspase activation by inhibiting inhibitor of apoptosis proteins, which are endogenous caspase inhibitors (1, 2). Mitochondrial membrane permeability is regulated by a group of proteins called the Bcl-2 family. This family of proteins can be divided into anti-apoptotic members (Bcl-2, Bcl-x_L, and Mcl-1) and pro-apoptotic members, which consist of multidomain members (Bak and Bax) and BH3-only proteins (Bid, Bim, Bik, Bad, Noxa, and Puma) (3, 4). Multidomain pro-apoptotic Bak and Bax are functionally redundant and play a direct role in increasing mitochondrial membrane permeability, leading to the release of apoptogenic proteins (5, 6). BH3-only proteins are thought to function as death signal sensors. After apoptotic stimulation, these proteins are primarily activated by different mechanism(s) and then activate Bak/Bax by still unknown mechanism(s) or inactivate anti-apoptotic Bcl-2 family members, finally leading to an increase of mitochondrial membrane permeability (3, 4).

Engagement of death receptors such as Fas and tumor necrosis factor α (TNFα)[1] receptor leads to one of two distinct apoptotic signaling pathways, which mainly differ in the extent of caspase-8 activation. In type I cells, there is extensive caspase-8 activation, which is sufficient to activate downstream execution caspases such as caspase-3 or caspase-7 and commit the cell to apoptotic death. In type II cells, there is less caspase-8 activation, so mitochondrial amplification of the apoptotic signal is required (7). In the latter type of cell, activated caspase-8 cleaves and activates a BH3-only protein, Bid (8, 9), which conveys apoptotic signals to the mitochondria by activating pro-apoptotic Bax or Bak (10–12). Because Bax and Bak are constitutively expressed, and the amount of these proteins usually remains unchanged during apoptosis, it is believed that Bak or Bax activation is regulated at the post-translational level (3, 13, 14). Bax is localized in the cytoplasm of living cells: after apoptotic stimulation, Bax translocates to the outer mitochondrial membrane where it oligomerizes and induces the formation of protein-conducting pores that release apoptogenic proteins (3, 12, 15–17). Bak is present on the outer mitochondrial membrane in a latent form: after accepting an upstream apoptotic signal, it undergoes oligomerization and induces the release of apoptogenic molecules from the mitochondria (11, 18).

Concealed epitopes at the N terminus of Bax or Bak are revealed after apoptotic stimulation, suggesting that a conformational change occurs in Bax and Bak or that a binding protein (which masks the N terminus) undergoes dissociation

* This work was supported by a grant for Scientific Research on Priority Areas, a grant for Center of Excellence Research, a grant for Scientific Research from the Ministry of Education, Science, Sports, and Culture of Japan, and by Special Coordination Funds for Promoting Science and Technology from the Science and Technology Agency of Japan. The costs of publication of this article were defrayed in part by the payment of page charges. This article must therefore be hereby marked "*advertisement*" in accordance with 18 U.S.C. Section 1734 solely to indicate this fact.

¶ To whom correspondence should be addressed. Tel.: 81-6-6879-3363; Fax: 81-6-6879-3369; E-mail: tsujimot@gene.med.osaka-u.ac.jp.

[1] The abbreviations used are: TNF, tumor necrosis factor; DSS, disuccinimidyl suberate; BMH, bismaleimidohexane; FBS, fetal bovine serum; MEF, mouse embryonic fibroblast; PBS, phosphate-buffered saline; CHAPS, 3-[(3-cholamidopropyl)dimethylammonio]-1-propanesulfonic acid; siRNA, small interference RNA; GFP, green fluorescent protein; STS, staurosporine; z-VAD-fmk, benzyloxycarbonyl-VAD-fluoromethyl ketone; FACS, fluorescence-activated cell sorting; ERK, extracellular signal-regulated kinase; JNK, c-Jun N-terminal kinase; rBid, recombinant human Bid.

(10, 13, 14, 19). Because it has been reported that exposure of the N terminus of Bax precedes its translocation to the mitochondria and oligomerization (12, 20), it seems that exposure of the N terminus of Bax or Bak represents an intermediate step leading to their activation. Oligomerization of Bax/Bak is thought to reflect its activation, because Bax/Bak oligomerizes after apoptotic stimulation, and this process is correlated precisely with the release of cytochrome *c*, and oligomerized Bax, but not monomeric Bax, induces cytochrome *c* releasing from the isolated mitochondria (11, 12, 15, 21). However, the process of regulation of the activation of Bak during apoptosis, and the relationship between exposure of the N terminus of Bak and oligomerization in the activation process, are still unclear.

In the present study, we found that Fas stimulation elicited a caspase-8-independent signal that induced exposure of the N terminus of Bak. This N-terminal exposure was not sufficient for full activation of Bak, but primed it to become more sensitive to apoptotic signals causing full activation.

EXPERIMENTAL PROCEDURES

Antibodies and Reagents—Anti-Bak (Ab1) monoclonal antibody was purchased from Oncogene Research Products (Boston, MA). Anti-Bax (N20) and anti-Bid polyclonal antibodies were obtained from Santa Cruz Biotechnology (Santa Cruz, CA) and R&D System (Minneapolis, MN), respectively. Anti-cytochrome *c* (6H2 and 7H8) and anti-mouse-Fas (Jo2) monoclonal antibodies were from BD Pharmingen. Anti-human Fas (CH11), anti-caspase-3, and anti-caspase-8 monoclonal antibodies were obtained from MBL (Nagoya, Japan). Anti-glyceraldehyde-3-phosphate dehydrogenase and anti-porin (voltage-dependent anion channel protein) monoclonal antibodies were obtained from Chemicon (Temecula, CA) and Calbiochem (San Diego, CA), respectively. All of the secondary antibodies were purchased from Molecular Probes (Eugene, OR).

The cross-linkers disuccinimidyl suberate (DSS) and bismaleimidohexane (BMH) were from Pierce Biotechnology (Rockford, IL). Other chemicals were obtained from Sigma. Recombinant human Bid (rBid) was prepared as described previously (22).

Cell Culture—The human HeLa cell line, human Jurkat T-leukemic cell line and Jurkat caspase-8-deficient subline (JB6) (23) were grown in RPMI 1640 medium supplemented with 10% fetal bovine serum (FBS). Mouse embryonic fibroblasts (MEFs) derived from caspase-8-deficient mice were grown in Dulbecco's modified Eagle's medium supplemented with 10% FBS.

Immunofluorescence Staining—Cells were fixed in 4% paraformaldehyde for 30 min and then permeabilized with 0.1% Triton X-100 for 15 min at room temperature. After incubation with 2% FBS in phosphate-buffered saline (PBS) for 1 h, the cells were incubated with anti-Bak (Ab1) (1:500) or anti-cytochrome *c* (1:500) for 1 h. After washing three times with PBS, the cells were incubated with the secondary antibody (Alexa 488-conjugated anti-mouse IgG) for 1 h. Then fluorescence was detected under a confocal microscope (Zeiss, LSM510).

Jurkat cells were fixed, permeabilized, and blocked with 20% FBS in PBS and then incubated with anti-Bak (Ab1) antibody followed by a secondary antibody (Alexa 568-conjugated anti-mouse IgG). The cells were subsequently analyzed by a flow cytometer (BD Biosciences, FACSCalibur) or observed under a confocal fluorescence microscope. In all immunostaining experiments, normal mouse IgG was added instead of the primary antibody (IgG) as a negative control.

Analysis of Cell Death—Cell viability was detected by staining with Annexin-V or Hoechst 33342. Briefly, cells were stained with Cy3-conjugated Annexin-V or 1 μM Hoechst 33342 for 5 min at room temperature and then analyzed using a flow cytometer or examined under a fluorescence microscope (Olympus, BX50).

Gel Filtration Analysis—Jurkat cells were treated, harvested, and extracted with HNC buffer (25 mM HEPES (pH7.5), 300 mM NaCl, 1 mM dithiothreitol, 2% CHAPS). The extracts were applied to a Superdex 200 HR 10/30 column (Amersham Biosciences), and fractions (40 μl) were collected for analysis by Western blotting. In some experiments, extracts were incubated with anti-Bak (Ab1) antibody or normal mouse IgG for 3 h before being applied to the column.

Cross-linking—Jurkat cells were harvested, incubated with 1 mM or 0.1 mM BMH for 30 min at room temperature, and then incubated with 1 mM dithiothreitol for 15 min to quench the cross-linker. Next, the cells were solubilized in sample buffer and analyzed by Western blotting. When the cross-linker DSS was used, Jurkat cells were lysed with HNC buffer, and then the lysates were incubated with 1 mM DSS for 30 min at room temperature, followed by incubation with 100 mM Tris buffer (pH 7.4) for 15 min to quench the cross-linker. As a control, the same concentration of Me_2SO was added instead of reagents.

siRNA Study—All siRNAs were produced by Dharmacon Research, and their sequences were as follows (numbers in parentheses indicate nucleotide positions within the respective open reading frame): mouse Bak (65–85), 5′-AACAGCAGGUUGCCCAGGACA-3′; mouse Bax (231–252), 5′-AGGAUGAUUGCUGACGUGGAC-3′; and GFP (274–294), 5′-GGCUACGUCCAGGAGCGCACC-3′. Cells were transfected with siRNA by electroporation using an Amaxa System three times at 48-h intervals.

Permeabilized Cells—HeLa cells were cultured in 10-well glass slides. After washing twice with isotonic buffer (20 mM Hepes-KOH (pH 7.4), 1.5 mM $MgCl_2$, 10 mM KCl, 250 mM sucrose), the cells were incubated with isotonic buffer containing 20 μg/ml digitonin for 3 min at room temperature. After washing three times with isotonic buffer, the cells were incubated with cytosol or rBid for 10 min at 37 °C. After washing another three times with isotonic buffer, the cells were subjected to immunostaining.

Preparation of Cytosol—After washing three times with isotonic buffer, cells were suspended in the same volume of isotonic buffer supplemented with protease inhibitors, and then homogenized using a Dounce homogenizer. After centrifugation at 100,000 × *g* for 1 h, the supernatant was obtained and used as the cytosol.

Subcellular Fractionation—Cells were fractionated as described previously (24). Briefly, cells were harvested, washed three times with isotonic buffer, and then incubated with 30 μg/ml digitonin in isotonic buffer for 5 min at 37 °C. After centrifugation at 3000 rpm for 3 min, aliquots of the supernatant (cytosolic fractions) and the pellet (containing the mitochondria) were analyzed by Western blotting with an anti-cytochrome *c* antibody.

In Vitro Analysis of Cytochrome c Release—Mitochondria were prepared from the livers of male Donryu rats as described previously (25). Briefly, the livers were harvested and homogenized in buffer A (0.3 M mannitol, 10 mM potassium Hepes (pH 7.4), 0.1% fatty acid-free bovine serum albumin, 0.2 mM EDTA) with a glass-Teflon Potter homogenizer. Then isolated mitochondria (100 μg of protein) were suspended in buffer B (buffer A plus 100 μM potassium phosphate and 4.3 mM succinate instead of EDTA) and incubated with 5 μl (40 μg of protein) of cytosol or with isotonic buffer for 5 min at room temperature, followed by incubation with or without rBid (30 μg) for a further 20 min. The mitochondria were collected by centrifugation (15,000 rpm, 5 min), and the supernatant was analyzed by Western blotting with an anti-cytochrome *c* antibody.

RESULTS

Caspase-independent Exposure of the N Terminus of Bak Occurs in Fas-stimulated Cells—Using a monoclonal antibody (anti-Bak Ab1) that recognized the N-terminal epitope of human Bak, we examined whether there were any changes to the N terminus of Bak in HeLa cells treated with an agonistic anti-Fas antibody, CH11. As reported previously (13, 19), Bak could not be recognized in living cells by Ab1 antibody, whereas cells exhibited increased immunoreactivity to Ab1 antibody after Fas stimulation (Fig. 1, *A* and *B*). Because we could not detect any change of Bak protein content after treatment with CH11 (Fig. 1*C*), this increased immunoreactivity to Ab1 antibody indicated exposure of the N terminus of Bak. Exposure of the N terminus could be detected after 1 h of treatment with CH11, when only a few cells had died (Fig. 1, *B* and *D*), consistent with the findings of others that exposure of the N terminus was an early event occurring before morphological changes (13, 19).

In HeLa cells (type II cells), Fas stimulation initiates the activation of caspase-8, which cleaves Bid, a pro-apoptotic member of the Bcl-2 family, and truncated Bid translocates to the mitochondria and activates Bak or Bax by a still unidentified mechanism (9–11). To investigate whether caspase-8 is involved in exposure of the N terminus of Bak, we employed a broad spectrum caspase inhibitor (z-VAD-fmk) to suppress caspase activation. Unexpectedly, we found that z-VAD-fmk (100 μM) did not affect the increased immunoreactivity to Ab1

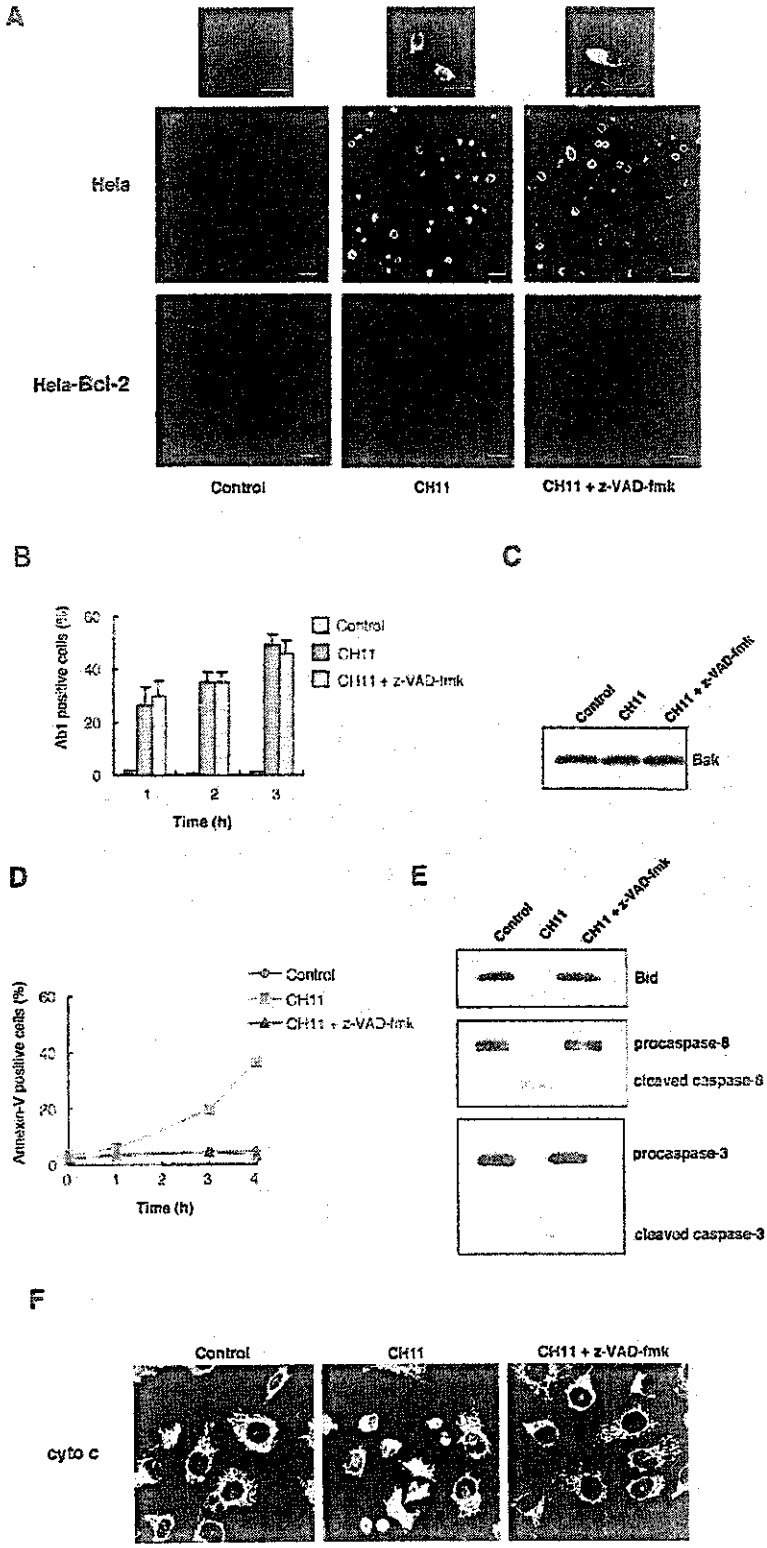

FIG. 1. **CH11-induced exposure of the N terminus of Bak in the presence of z-VAD-fmk.** *A* and *B*, HeLa cells and HeLa cells overexpressing Bcl-2 (HeLa-Bcl-2) were treated without or with CH11 (0.5 μg/ml) for 4 h (*A*) or for the indicated times (*B*) in the presence or absence of z-VAD-fmk (100 μM). Cells were immunostained with a monoclonal anti-Bak Ab1 antibody. *A*, representative images are shown. *Scale bar* = 20 μm. *Top*: enlarged images of immunostaining. *B*, Ab1-positive cells from four randomly chosen fields were counted under a confocal microscope. Data are shown as the mean ± S.E. (n = 3). *C*, Western blot analysis of Bak from HeLa cells treated as indicated for 4 h. *D*, inhibition of CH11-induced apoptosis of HeLa cells by z-VAD-fmk. *E*, inhibition by z-VAD-fmk of cleavage of Bid and the activation of caspase-8 and caspase-3 in HeLa cells. HeLa cells were treated without or with CH11 (0.5 μg/ml) in the presence or absence of z-VAD-fmk (100 μM) for 8 h and then subjected to Western blot analysis with the indicated antibodies. *F*, inhibition of CH11-induced release of cytochrome *c* by z-VAD-fmk. HeLa cells were treated without or with CH11 (0.5 μg/ml) in the presence or absence of z-VAD-fmk (100 μM) for 4 h and then immunostained with a monoclonal anti-cytochrome *c* antibody.

antibody in CH11-treated cells (Fig. 1, *A* and *B*), although the dose of z-VAD-fmk that we used could almost completely suppress the activation of caspases-8, cleavage of Bid, release of cytochrome *c* from the mitochondria, activation of caspase-3, and cell death (Fig. 1, *D–F*).

Because Bcl-2/Bcl-x_L is known to inhibit the activation of Bax and Bak (26, 27), we also examined whether CH11-induced exposure of the N terminus of Bak was inhibited by Bcl-2. As shown in Fig. 1*A*, overexpression of Bcl-2 completely inhibited exposure of the N terminus of Bak in CH11-treated cells with or without exposure to z-VAD-fmk.

We next tested whether the same phenomenon also occurred